SELF-NOISE IN INTERFEROMETERS: RADIO AND INFRARED

SHRINIVAS R. KULKARNI[a)]
Owens Valley Radio Observatory and Palomar Observatory, California Institute of Technology, 105-24, Pasadena, California 91125
Received 26 January 1989; revised 11 April 1989

ABSTRACT

The quality of images obtained from modern radio synthesis arrays is, under the best conditions, limited only by the noise generated by the receiving circuitry and extraneous radiation from a variety of background sources. We present a complete theory of the noise in a synthesis image valid for a source of *arbitrary* strength. The analysis presented here gives a deeper understanding of coherence theory as applied to astronomical imaging. In the limit of faint sources, we recover the standard estimates of noise in a synthesis image. In the opposite limit of a strong source we show that the noise in the synthesis image is dominated by self-noise, or the noise generated by the source signal itself. We extend our theory to imaging by the use of closure phase or the bispectrum. Application of our theory to large, low-noise arrays like the VLA, the planned Indian GMRT, or VLBI show that a fair number of sources are bright enough that self-noise is an important source of noise. We present formal expressions of self-noise in synthesis maps and show that the distribution of self-noise is not uniform across the map. We suggest that some of the best VLBI maps, with noise approaching the thermal noise, may in fact be limited by self-noise. We also show that there is a bias in the standard definition of the bispectrum phasor and hence the closure phase as well. Fortunately, this bias is negligible. Finally, we resolve some of the conceptual difficulties associated with the hybrid mapping procedure and suggest contrary to the established procedure that *all* closure phases carry information and there are no "basic" closure phases. In particular, we suggest that at low signal levels, characteristic of infrared interferometers, it is best to fit the model to all the closure phases and fringe amplitudes.

I. INTRODUCTION

Interferometric imaging or synthesis imaging is now a commonly used astronomical technique, especially at radio wavelengths. Modest technological gains coupled with advances in imaging theory have enabled astronomers to routinely obtain high-quality images from modern radio synthesis arrays like the Very Large Array (VLA). The eventual limitation to the dynamic range of a synthesis image is set by the uncertainties or the noise in the measurement of the visibility function. The noise arises from the receiving electronics, and radiation from the ground, the sky, etc. This issue, the signal-to-noise ratio (SNR) in the synthesized image, has been treated in detail by several authors (e.g., see Thompson, Moran, and Swenson 1986, and references therein).

A typical radio interferometer array consists of n antennas, each equipped with a low-noise receiver. Cosmic signal collected by each antenna is amplified by the receiver electronics and sent over to a central facility. In the central facility, the n signals are brought to a common "focus" by the delay and the phase compensation circuitry and then fed to a correlator system wherein the n signals are multiplied pairwise and averaged, resulting in $n_b = n(n-1)/2$ complex fringe amplitudes. These n_b complex numbers (also referred to as the fringe phasors) are estimates of the spatial coherence function of the astronomical image at the spatial frequencies determined by the vectors connecting pairs of antennas. Rotation due to Earth or actual transportation of the antennas enables measurement of additional spatial-frequency components. Once sufficient spatial-frequency components have been measured the astronomical source is "synthesized" by Fourier transforming the measured spatial coherence function (the van Cittert–Zernike theorem).

The principal source of noise in a radio interferometer is that due to the noise generated by the receiver electronics. Other sources of noise include the 3 K cosmic background radiation, the Galactic synchrotron radiation, and radiation from the ground, the telescope structure, and the atmosphere leaking through the sidelobes of the radio telescope. All these sources of noise are usually lumped in one category and collectively referred to as the receiver noise N. The receiver noise can be considered a purely additive noise. The receiver noise is related to T_R, the antenna temperature measured in the absence of a strong source by the relation $N = \frac{1}{2}kT_R/\eta A$, where A is the geometrical collecting area of the telescope ($\pi D^2/4$) and η is the so-called aperture efficiency. N is thus the noise equivalent flux density (NEFD) in the terminology of infrared astronomy. A typical VLA antenna, in the centimeter window, has $T_R \sim 50$ K and $\eta \sim 0.6$, and thus $N \sim 480$ Jy. In contrast, an astronomical source with flux density $S = 10$ Jy is considered to be a rather bright source. Thus, for most sources, the principal source of noise in the measurement of the fringe phasors is determined mainly by receiver noise N.

Standard aperture synthesis noise analysis discussed in literature takes advantage of the low value of S/N. However, improvements in receiver technology could decrease substantially N, e.g., the 40 m Green Bank telescope of NRAO has a $T_R = 25$ K in the 1.4 GHz band and thus $N = 96$ Jy. Also, the *total* collecting area of modern arrays such as the VLA or the planned Indian GMRT (Giant Meter Wavelength Telescope) is substantial. Both these effects increase the noise in the synthesized images beyond what is estimated from the standard asymptotic calculations (e.g., Crane and Napier 1985; Thompson *et al.* 1986, Chap. 6). The excess noise in the measurement of the fringe phasors results from the source itself and has been termed as "self-noise." Self-noise has been previously discussed in the context of single-dish measurements.

[a)] Alfred P. Sloan Fellow and Presidential Young Investigator.

 0004-6256/89/031112-19$00.90

In this paper, we present a complete analysis of the noise in images produced by the synthesis technique, valid for sources of *arbitrary* strength. In the asymptotic limit of low S/N, our analysis reproduces the conventional result. Some surprises are seen for bright sources. The analysis presented leads to deeper understanding in coherence theory as applied to astronomical imaging and provides formulations that can be immediately applied to strong-source mapping.

Radio interferometers belong to a general class of interferometers—the "coherent" interferometers employing the heterodyne technique—as opposed to interferometers at optical wavelengths, which combine the beams from different antennas directly and the fringe pattern is detected by "incoherent" detectors. Heterodyne interferometry is neither advantageous nor feasible at optical wavelengths. However, in the infrared, especially the far infrared, heterodyne interferometers employing very low-noise receivers may be superior to homodyne interferometers. The analysis presented here is applicable to all heterodyne interferometers that are dominated by additive noise.

The van Cittert–Zernike theorem, the basis of synthesis imaging, presupposes no corruption of the astronomical signal. However, the atmosphere certainly affects the signal at IR wavelengths. At radio wavelengths, atmospheric corruption, if uncorrected, limits the dynamic range (small baselines like the VLA) or even precludes image construction (long baselines as in VLBI). In these situations, the use of the closure phases or the bispectrum enables image construction (see Pearson and Readhead 1984). Given the importance of imaging based on the bispectrum, especially in the IR window, we have extended our analysis to the noise in images constructed using the bispectrum. This analysis is also of some importance to synthesis imaging of faint radio sources.

The organization of this paper is as follows. In Sec. II, we discuss the assumptions inherent to this analysis. Based on these assumptions, we estimate the uncertainty in the fringe amplitude (Sec. III). In Sec. IV, we estimate the covariance of pairs of fringe phasors. We then estimate the SNR in the synthesized image for a simple source (a point source at phase center) in Sec. V. We derive the statistical properties of the bispectrum phasors in Sec. VI. In Sec. VII, we present the SNR analysis of images synthesized from bispectrum data. We apply the results of our analysis to three examples: strong-source mapping at the VLA, VLBI imaging, and faint-object imaging at IR wavelengths (Sec. VIII). Recognizing that most readers may not wish to read all the details, we summarize all the important results and formulas in Sec. IX.

II. THEORETICAL BASIS

We assume that the principal source of noise in a radio interferometer is an additive noise. In reality, other sources of noise such as imperfect quadrature networks, noise introduced by correlators, etc., can be significant and may eventually limit the dynamic range of modern synthesis images (see Perley 1985). However, these errors can be diminished with improvements in technology and hence we ignore them. We also assume that there is no atmospheric corruption of the cosmic signal. Noise analysis in the presence of atmospheric corruption is treated in Secs. VI and VII.

For simplicity, we assume that the synthesis array consists of n identical antennas. Let voltage s_j be the astronomical signal received by antenna j and voltage n_j be the additive noise from the same antenna; here $j = 1,...,n$. As explained above, the additive noise arises from noisy receivers, antenna spillover, etc. Both s_j and n_j are assumed to be zero-mean, complex Gaussian random variables.

The astronomical signal is coherent and thus we expect s_j and s_k to be correlated. In particular, we assume (for $j \neq k$)

$$\langle \mathrm{Re}\,(s_j)\ \mathrm{Re}\,(s_k)\rangle = +\tfrac{1}{2}|R_{jk}|\cos(\phi_{jk}), \tag{1a}$$

$$\langle \mathrm{Re}\,(s_j)\ \mathrm{Im}\,(s_k)\rangle = +\tfrac{1}{2}|R_{jk}|\sin(\phi_{jk}), \tag{1b}$$

$$\langle \mathrm{Im}\,(s_j)\ \mathrm{Re}\,(s_k)\rangle = -\tfrac{1}{2}|R_{jk}|\sin(\phi_{jk}), \tag{1c}$$

$$\langle \mathrm{Im}\,(s_j)\ \mathrm{Im}\,(s_k)\rangle = +\tfrac{1}{2}|R_{jk}|\cos(\phi_{jk}), \tag{1d}$$

and for $j = k$

$$\langle \mathrm{Re}\,(s_j)\ \mathrm{Re}\,(s_j)\rangle = \tfrac{1}{2}S, \tag{1e}$$

$$\langle \mathrm{Re}\,(s_j)\ \mathrm{Im}\,(s_j)\rangle = 0, \tag{1f}$$

$$\langle \mathrm{Im}\,(s_j)\ \mathrm{Re}\,(s_j)\rangle = 0, \tag{1g}$$

$$\langle \mathrm{Im}\,(s_j)\ \mathrm{Im}\,(s_j)\rangle = \tfrac{1}{2}S, \tag{1h}$$

where S is the flux density of the source. Note that S, unlike N, is independent of the collecting area of the antenna. R_{jk} and ϕ_{jk} are the correlated flux or the fringe amplitude and the fringe phase on baseline jk, respectively. The angular brackets $\langle\ \rangle$ refer to *ensemble* average.

The receiver-noise components, owing to their origin in separate receivers, etc., are assumed to be uncorrelated with each other, i.e.,

$$\langle \mathrm{Re}\,(n_j)\ \mathrm{Re}\,(n_k)\rangle = \langle \mathrm{Re}\,(n_j)^2\rangle\delta_{jk} = \tfrac{1}{2}N\delta_{jk}, \tag{2a}$$

$$\langle \mathrm{Re}\,(n_j)\ \mathrm{Im}\,(n_k)\rangle = 0, \tag{2b}$$

$$\langle \mathrm{Im}\,(n_j)\ \mathrm{Re}\,(n_k)\rangle = 0, \tag{2c}$$

$$\langle \mathrm{Im}\,(n_j)\ \mathrm{Im}\,(n_k)\rangle = \langle \mathrm{Im}\,(n_j)^2\rangle\delta_{jk} = \tfrac{1}{2}N\delta_{jk}, \tag{2d}$$

where N is the receiver-noise power per antenna.

From Eqs. (1) and (2) we see that the flux density of the source and the receiver-noise power of any antenna are, respectively, per polarization,

$$S = \langle s_j s_j^* \rangle, \tag{3a}$$

$$N = \langle n_j n_j^* \rangle. \tag{3b}$$

Finally, the receiver noise and the astronomical signals are independent and hence are uncorrelated to all orders. In particular,

$$\langle \mathrm{Re}\,(n_j)\ \mathrm{Re}\,(s_k)\rangle = \langle \mathrm{Re}\,(n_j)\rangle\langle \mathrm{Re}\,(s_k)\rangle = 0, \quad \text{etc.}, \tag{4}$$

for all j, k.

It is important to note that the above relations (1)–(4) are valid only when the signal and noise amplitudes are measured at the same instant. We now consider the analogs of Eqs. (1)–(4) for voltages measured at different times.

Let B be the bandwidth of the signal; clearly, the bandwidth of the receiver noise is also B. We assume that the signals are sampled at the Nyquist rate $2B$. The finite bandwidth introduces temporal correlations, and these can be effectively taken into account by the assumption that the voltage samples are correlated with each other only over a time interval equal to the sampling interval $\tau_c \sim (2B)^{-1}$ and are completely decorrelated for time intervals exceeding τ_c, i.e.,

$$\langle \mathrm{Re}\,(s_j^p)\ \mathrm{Re}\,(s_k^q)\rangle = \langle \mathrm{Re}\,(s_j)\ \mathrm{Re}\,(s_k)\rangle\delta_{pq} = \tfrac{1}{2}|R_{jk}|\cos(\phi_{jk})\delta_{pq}, \tag{5}$$

where s_j^p refers to the signal from antenna j measured at

$t = p\tau_c$. Similar relations follow for the other combinations of the real and imaginary components of the astronomical signals [cf. Eqs. (1)]. For the receiver-noise components, using Eqs. (2) and the above assumptions, we find

$$\langle \mathrm{Re}\,(n_j^p)\ \mathrm{Re}\,(n_j^q)\rangle = \tfrac{1}{2}N\delta_{pq}\delta_{jk}. \tag{6}$$

Again, similar relations follow for other combinations of the real and imaginary components of the receiver noise [cf. Eqs. (2)].

The mean complex fringe visibility is by definition

$$R_{jk} \equiv \langle r_{jk}\rangle = \langle (s_j + n_j)(s_k^* + n_k^*)\rangle. \tag{7}$$

Operationally, the mean fringe visibility is obtained in two steps. In the first step, signals from pairs of antennas are correlated and the resulting correlation summed over a certain interval τ_I to yield *one* measurement r_{jk} of the mean fringe visibility,

$$r_{jk} = 1/M \sum_{p=1}^{M} (s_j^p + n_j^p)(s_k^{p^*} + n_k^{p^*}). \tag{8a}$$

Here $M = 2B\tau_I$ is the number of independent voltage samples in the interval τ_I. τ_I is usually set to the coherence integration interval τ_{coh} (Sec. VI) and is at least several tens of seconds at centimeter wavelengths. Thus, for a modest value of $\tau_I \sim 10$ s and assuming $B \sim 100$ MHz, $M = 10^9$—a very large number.

The second step is to average many r_{jk}'s to obtain R_{jk}, i.e.,

$$R_{jk} = \overline{r_{jk}}, \tag{8b}$$

where the bar indicates a temporal average. It is usual to assume that the signal and noise components are ergodic, i.e., temporal averaging and ensemble averages are completely equivalent. We make frequent appeal to this assumption. This assumption allows us to rewrite Eq. (8b) as

$$R_{jk} = 1/M \sum_{p=1}^{M} \langle (s_j^p + n_j^p)(s_k^{p^*} + n_k^{p^*})\rangle. \tag{8c}$$

This step allows us great simplifications. In particular, application of Eqs. (1)–(4) yields

$$\begin{aligned} R_{jk} &= 1/M \sum_{p=1}^{M} \langle \mathrm{Re}\,(s_j^p)\ \mathrm{Re}\,(s_k^p)\rangle + \langle \mathrm{Im}\,(s_j^p)\ \mathrm{Im}\,(s_k^p)\rangle \\ &\quad + i[\langle \mathrm{Im}\,(s_j^p)\ \mathrm{Re}\,(s_k^p)\rangle - \langle \mathrm{Re}\,(s_j^p)\ \mathrm{Im}\,(s_k^p)\rangle] \\ &= \langle \mathrm{Re}\,(s_j)\ \mathrm{Re}\,(s_k)\rangle + \langle \mathrm{Im}\,(s_j)\ \mathrm{Im}\,(s_k)\rangle \\ &\quad + i\langle \mathrm{Im}\,(s_j)\ \mathrm{Re}\,(s_k)\rangle - i\langle \mathrm{Re}\,(s_j)\ \mathrm{Im}\,(s_k)\rangle \\ &= R_{jk}[\cos(\phi_{jk}) - i\sin(\phi_{jk})]. \end{aligned} \tag{8d}$$

III. UNCERTAINTY IN THE FRINGE AMPLITUDE

We now determine the uncertainty in the fringe amplitude. For specificity we assume the fringe phasor on baseline 12. The fringe phasor consists of two components: real and imaginary. Rather than evaluating the variances of these two components, we evaluate the following "pseudovariance,"

$$\begin{aligned} \sigma^2_{R_{12}} &\equiv \langle r_{12} r_{12}^*\rangle - \langle r_{12}\rangle\langle r_{12}^*\rangle \\ &= \frac{1}{M^2}\sum_{p=1}^{M}\sum_{q=1}^{M}[\langle (s_1^p + n_1^p)(s_2^{p^*} + n_2^{p^*}) \\ &\quad \times (s_1^{q^*} + n_1^{q^*})(s_2^q + n_2^q)\rangle] - R_{12}R_{12}^*. \end{aligned} \tag{9}$$

The variances of the real and the imaginary components can be found in Appendix B.

There are 16 fourth-order terms in the square brackets in Eq. (9): $s_1^p s_2^{p^*} s_1^{q^*} s_2^q$, $s_1^p s_2^{p^*} s_1^{q^*} n_2^q$,..., $n_1^p n_2^{p^*} n_1^{q^*} n_2^q$. Of these 16 terms, owing to Eq. (5), only terms that do not involve any noise components such as $s_1^p s_2^{p^*} s_1^{q^*} s_3^q$ or pairs of noise components from the same antenna such as $s_1^p n_2^{p^*} s_1^{q^*} n_2^q$ are nonzero. Thus Eq. (9) simplifies to

$$\begin{aligned} \sigma^2_{R_{12}} &= \frac{1}{M^2}\sum_{p=1}^{M}\sum_{q=1}^{M}[\langle s_1^p s_2^{p^*} s_1^{q^*} s_2^q\rangle + \langle s_1^p n_2^{p^*} s_1^{q^*} n_2^q\rangle \\ &\quad + \langle n_1^p s_2^{p^*} n_1^{q^*} s_2^q\rangle + \langle n_1^p n_2^{p^*} n_1^{q^*} n_2^q\rangle] - R_{12}R_{12}^*. \end{aligned} \tag{10}$$

Equation (10) can be further simplified by the application of the well-known fourth-moment theorem for real Gaussian random variables (Davenport and Root 1958, p. 168):

$$\begin{aligned} \langle x_1 x_2 x_3 x_4\rangle &= \langle x_1 x_2\rangle\langle x_3 x_4\rangle + \langle x_1 x_3\rangle\langle x_2 x_4\rangle \\ &\quad + \langle x_1 x_4\rangle\langle x_2 x_3\rangle. \end{aligned} \tag{11}$$

In Appendix A, we extend this theorem for complex Gaussian variables and in addition show that all second-order products of the form $\langle z_j z_k\rangle$ (or its conjugate) are identically zero. Utilizing these results as well as Eqs. (3) and (4) allows us the following simplifications:

$$\begin{aligned} \langle s_1^p s_2^{p^*} s_1^{q^*} s_2^q\rangle &= \langle s_1^p s_2^{p^*}\rangle\langle s_1^{q^*} s_2^q\rangle + \langle s_1^p s_1^{q^*}\rangle\langle s_2^{p^*} s_2^q\rangle \\ &= R_{12}R_{12}^* + S^2\delta_{pq}, \\ \langle s_1^p n_2^{p^*} s_1^{q^*} n_2^q\rangle &= \langle s_1^p s_1^{q^*}\rangle\langle n_2^{p^*} n_2^q\rangle = SN\delta_{pq}, \\ \langle n_1^p s_2^{p^*} n_1^{q^*} s_2^q\rangle &= \langle n_1^p n_1^{q^*}\rangle\langle s_2^{p^*} s_2^q\rangle = SN\delta_{pq}, \\ \langle n_1^p n_2^{p^*} n_1^{q^*} n_2^q\rangle &= \langle n_1^p n_1^{q^*}\rangle\langle n_2^{p^*} n_2^q\rangle = N^2\delta_{pq}. \end{aligned}$$

Thus

$$\sigma^2_{R_{12}} = (S^2 + 2NS + N^2)/M = (S + N)^2/M. \tag{12}$$

Hence, the pseudovariance of the fringe phasor on any baseline is proportional to the square of the *total* power, i.e., receiver noise plus signal, and inversely proportional to M, the $B\tau_I$ product.

Consider two asymptotic limits of Eq. (12):

Weak source (S≪N). In this limit

$$\sigma_{R_{12}} = \frac{N}{\sqrt{2B\tau_I}}. \tag{13a}$$

This is the standard result quoted in the literature and shows that in the faint-source limit the principal source of noise in the measurement of a fringe phasor is the additive receiver noise.

Strong source (S≫N). In this limit

$$\sigma_{R_{12}} = \frac{S}{\sqrt{2B\tau_I}}. \tag{13b}$$

This is a well-known result in the context of flux-density measurement using a single dish. Equation (13b) shows that when the source power overwhelms the additive receiver-noise power, the uncertainty in the fringe amplitude is proportional to the source flux density and thus the SNR is *independent of the source flux density and depends only on the $B\tau_I$ product.* Again, this is expected since, over an interval τ_I, there are only $\sim B\tau_I$ independent samples in a band-limited signal. Thus the best SNR that we can extract for the fringe amplitude or, for that matter, any other quantity is $\sim\sqrt{B\tau_I}$.

IV. COVARIANCE OF FRINGE AMPLITUDES

An n-element interferometer yields $n_b = n(n-1)/2$ complex fringe amplitudes and n total-power measurements

every integration time τ_I. It is commonly assumed that the n_b fringe phasors constitute independent measurements of the spatial coherence function. Thus the SNR in the synthesized image is supposed to scale as $\sim\sqrt{n_b}\sim n$ (e.g., Crane and Napier 1985; Thompson *et al.* 1986, Chap. 6). However, this assumption cannot be correct since there are only n independent noise components and n signal terms. The n signal terms are not completely independent; in fact, the spatial coherence function of a point source is unity for all separations! Hence, it is impossible to derive $\sim n^2$ independent quantities from essentially $\lesssim 2n$ independent sources. Thus we expect, on general grounds, that the noise in the measurements of the n_b fringe phasors ought to be correlated with each other. In this section we estimate the degree of correlation between pairs of fringe phasors.

The map or the image is the Fourier transform of the measured visibilities, i.e., each pixel in the map is a linear combination of the measured visibilities. Thus, it is sufficient to estimate the *first order* or linear correlation between pairs of fringe phasors in order to estimate the SNR in the map. The linear correlation between two random variables x, y is best measured by the covariance element $C_{xy}\equiv\langle xy\rangle-\langle x\rangle\langle y\rangle$ or the related quantity, the normalized covariance, $\mu_{xy}\equiv C_{xy}/\sigma_x\sigma_y$, where $\sigma_x^2\equiv C_{xx}$, etc. The absolute value of the normalized covariance varies between 0 and 1.

We take a brief digression to clarify the difference between independent and uncorrelated random variables. x and y are *independent* variables if they are uncorrelated to all orders, i.e.,

$$\langle x^n y^m\rangle-\langle x^n\rangle\langle y^m\rangle=0 \quad \text{for all } n,m.$$

x and y are *uncorrelated* if $C_{xy}=0$. Independence is thus a stricter condition since it is possible for x and y to be uncorrelated but dependent, i.e., $x=\sin(\theta)$ and $y=\cos(\theta)$, where θ is uniformly distributed on $[0,2\pi]$. Only in the special case of Gaussian statistics are the terms independence and uncorrelated completely equivalent (Davenport and Root 1958, Chap. 8).

For an n-element interferometer there are n_b fringe phasors. Thus we need n_b^2 covariance elements to describe the correlation between all possible pairs of fringe phasors. These elements are best described by the covariance matrix C which is a square matrix of size $n_b\times n_b$. Element $C_{jk,j'k'}$ of this matrix is a measure of the linear correlation between the fringe phasors on baseline jk and $j'k'$. The matrix elements can be classified into three groups:

(1) Diagonal elements. The n_b diagonal terms are the variance of the fringe phasors: $C_{jk,jk}=\sigma^2_{R_{jk}}$.

(2) Nondiagonal elements of type "a." These measure the correlation between baselines that share a common antenna, e.g., baseline 12 and baseline 13.

(3) Nondiagonal elements of type "b." These measure the correlation between baselines that do *not* share any common antenna, e.g., baseline 12 and baseline 34.

Since a fringe phasor is composed of two components, real and imaginary, we need to evaluate all possible combinations, i.e., type "a" real–real, real–imaginary, imaginary–imaginary, and imaginary–real, and similarly for type "b" pairs. These combinations are evaluated in Appendix B. Here, for pedantic reasons, we evaluate a subset of the type "a" and "b" covariance elements and discuss their asymptotic limits.

We first consider a covariance element of type "a." For specificity, we assume baselines 12 and 13. Then,

$$C^a_{12,13}\equiv\langle r_{12}r^*_{13}\rangle-R_{12}R^*_{13}, \tag{14a}$$

where the superscript stresses that this is a type a covariance element. As before, we substitute temporal average for the ensemble average and obtain

$$C^a_{12,13}=\frac{1}{M^2}\sum_{p=1}^{M}\sum_{q=1}^{M}\langle(s_1^p+n_1^p)(s_2^{p*}+n_2^{p*})\times(s_1^{q*}+n_1^{q*})(s_3^q+n_3^q)\rangle-R_{12}R^*_{13}. \tag{14b}$$

The angular brackets in Eq. (14b) expand to 16 fourth-order averages: $s_1^p s_2^{p*}s_1^{q*}s_3^q,\ldots,n_1^p n_2^{p*}n_1^{q*}n_3^q$. Of these, owing to Eq. (4), only terms with no noise components ($s_1^p s_2^{p*}s_1^{q*}s_3^q$) or pairs of identical noise components ($n_1^p s_2^{p*}n_1^{q*}s_3^q$) are nonzero, yielding

$$C^a_{12,13}=\frac{1}{M^2}\sum_{p=1}^{M}\sum_{q=1}^{M}\langle s_1^p s_2^{p*}s_1^{q*}s_3^q\rangle+\langle n_1^p s_2^{p*}n_1^{q*}s_3^q\rangle-R_{12}R^*_{13} \tag{14c}$$

$$=(S+N)R^*_{23}/M, \tag{14d}$$

and the normalized covariance element is

$$\mu^a_{12,13}=R^*_{23}/(S+N), \tag{14e}$$

independent of M. Thus the normalized covariance is the ratio of the correlated flux density to the total power.

We now consider the asymptotic limits.

Weak source (S≪N). In this regime,

$$|\mu^a_{12,13}|=|R_{23}|/N=|\gamma_{23}|(\mathrm{S/N}), \tag{15a}$$

where $|\gamma_{23}|$ is the normalized fringe visibility and has the maximum value of unity (for a point source) and a minimum value of 0. Thus, even for a point source, in the weak source limit, pairs of fringe phasors involving a common antenna are approximately uncorrelated. This result makes sense since for a point source the astronomical signal is completely correlated and the only reason we get decorrelation is because receiver noise is uncorrelated. Thus the normalized covariance is the ratio of the correlated signal (i.e., S) to the uncorrelated signal (i.e., N).

Strong source (S≫N). In this regime,

$$|\mu^a_{12,13}|=|\gamma_{23}|. \tag{15b}$$

In this regime, the normalized covariance is equal to the normalized visibility on the baseline which does not involve the common antenna. Since for a point source $|\gamma_{jk}|=1$ for all j,k, pairs of fringe phasors that involve a common antenna are completely correlated. Again, this is expected because in this regime receiver noise is irrelevant and the correlation properties reflect the coherence properties of the astronomical source. Thus for a point source we expect and indeed find that the normalized covariance is unity. For an extended source, the normalized covariance is less than unity because the incident wavefront is curved and antennas j and k do not sample the same electric field at a given time.

We now evaluate covariance elements of type b. For specificity, we assume baselines 12 and 34 and as before we note

$$C^b_{12,34}=\frac{1}{M^2}\sum_{p=1}^{M}\sum_{q=1}^{M}\langle[(s_1^p+n_1^p)(s_2^{p*}+n_2^{p*})\times(s_3^{q*}+n_3^{q*})(s_4^q+n_4^q)]\rangle-R_{12}R^*_{34}, \tag{16a}$$

where the superscript b is a reminder to the reader that $C^b_{12,34}$ is a covariance element of type b. Owing to relation (4), only one fourth-order term of the 16 terms in the square brackets in Eq. (16a) is nonzero, yielding

$$C^{b}_{12,34} = R_{13}R^{*}_{24}/M, \tag{16b}$$

and the normalized covariance is

$$\mu^{b}_{12,34} = \frac{R_{13}}{(S+N)}\,\frac{R^{*}_{24}}{(S+N)}. \tag{16c}$$

We now consider the asymptotic limits.

Weak source (S≪N). In this limit,

$$|\mu^{b}_{12,34}| = |\gamma_{13}\gamma_{24}|(S/N)^2, \tag{17a}$$

which is even smaller than the corresponding case for pairs of baselines with a common antenna [cf. Eq. (15a)]. Equation (17a) can be anticipated from physical arguments. In the faint-source limit, any correlation between fringe phasors on unrelated baselines is via the astronomical signal and the decorrelation is due to the uncorrelated receiver noise. Correlated fluctuations of the two fringe phasors require identical fluctuations in the two fringe phasors and the covariance is thus a second-order process; hence the quadratic dependence on S/N in Eq. (17a).

Strong source (S≫N). In this limit,

$$|\mu^{b}_{12,34}| = |\gamma_{13}\gamma_{24}|. \tag{17b}$$

In this regime, the normalized covariance is a product of the normalized object visibilities on the two baselines. Consider now the special case of a point source ($|\gamma_{jk}| = 1$) in which case *the fringe phasors for pairs of baselines with no common station are completely correlated.* This happens because in the strong source limit the receiver noise is negligible and the coherence properties of the astronomical signal decide the covariance properties of the fringe phasors. For a point source, the incident wavefront is planar, which is fully correlated to any order.

V. NOISE IN THE SYNTHESIZED MAP

In this section we estimate the noise in the synthesized map. The synthesized map is the Fourier transform of the measured visibilities, i.e.,

$$i(\theta_x,\theta_y) = \frac{1}{n_b}\sum_{j=1}^{n}\sum_{j>k}^{n} a_{jk}(\theta_x,\theta_y)\,\mathrm{Re}\,(r_{jk}) + b_{jk}(\theta_x,\theta_y)\,\mathrm{Im}\,(r_{jk}). \tag{18a}$$

Denoting Re (r_{jk}) by r^{c}_{jk} and Im (r_{jk}) by r^{s}_{jk}, and applying a similar convention for the real and imaginary components of R_{jk}, we find that the mean value of the intensity at (θ_x,θ_y) is

$$I(\theta_x,\theta_y) = \langle i(\theta_x,\theta_y)\rangle = \frac{1}{n_b}\sum_{j=1}^{n}\sum_{j>k}^{n} a_{jk}(\theta_x,\theta_y)R^{c}_{jk} + b_{jk}(\theta_x,\theta_y)R^{s}_{jk}, \tag{18b}$$

where

$$a_{jk}(\theta_x,\theta_y) + ib_{jk}(\theta_x,\theta_y) = e^{i(u_j-u_k)\theta_x + i(v_j-v_k)\theta_y}.$$

Here θ_x,θ_y refer to the pixels in the map and u_j, v_j are the coordinates of antenna j (in some arbitrary coordinate system). The variance in the intensity of the map at pixel θ_x,θ_y is obtained from the standard error propagation of the right-hand side of Eqs. (18), i.e.,

$$\begin{aligned} V_I(\theta_x,\theta_y) &= \langle i^2(\theta_x,\theta_y)\rangle - \langle i(\theta_x,\theta_y)\rangle^2 \\ &= \frac{1}{n_b^2}\sum_{j=1}^{n}\sum_{k>j}^{n}\sum_{j'=1}^{n}\sum_{j'>k'}^{n} a_{jk}(\theta_x,\theta_y) \\ &\quad\times a_{j'k'}(\theta_x,\theta_y)C\,[r^{c}_{jk},r^{c}_{j'k'}] \\ &\quad + a_{jk}(\theta_x,\theta_y)b_{j'k'}(\theta_x,\theta_y)C\,[r^{c}_{jk},r^{s}_{j'k'}] \\ &\quad + b_{jk}(\theta_x,\theta_y)a_{j'k'}(\theta_x,\theta_y)C\,[r^{s}_{jk},r^{c}_{j'k'}] \\ &\quad + b_{jk}(\theta_x,\theta_y)b_{j'k'}(\theta_x,\theta_y)C\,[r^{s}_{jk},r^{s}_{j'k'}]. \end{aligned} \tag{19}$$

Here $C\,[r^{c}_{jk},r^{c}_{j'k'}]$, $C\,[r^{c}_{jk},r^{s}_{j'k'}]$, etc., are the covariance terms of the pair of fringe phasors R_{jk} and $R_{j'k'}$ and are evaluated in Appendix B. Equation (19) is the complete and formal expression for the variance in any desired pixel of a synthesized map.

In order to gain physical insight we consider a simple source, viz., a point source at the phase center for which $R_{jk} = 1$ for all j,k. We then evaluate the variance of the pixel at the phase center ($\theta_x = 0$, $\theta_y = 0$),

$$V_I(0,0) = \frac{1}{n_b^2}\sum_{j=1}^{n}\sum_{k>j}^{n}\sum_{j'=1}^{n}\sum_{j'>k'}^{n} C\,[\mathrm{Re}\,(r_{jk}),\mathrm{Re}\,(r_{j'k'})]. \tag{20}$$

Thus the variance of the pixel at the phase center is proportional to the sum of all the elements of the covariance matrix of the real components. As discussed in Sec. IV, the elements of the normalized covariance matrix can be divided into three types: (i) n_b diagonal elements whose value is unity, (ii) off-diagonal elements of type a, and (iii) off-diagonal elements of type b. For a point source, all the off-diagonal elements (both real and imaginary) of type a are equal to $\mu^a \sim S/(S+N)$ [Eq. (14e)] and that of type b are equal to $\mu^b = [S/(S+N)]^2$ [Eq. (16c)]. All that remains to evaluate $V_I(0,0)$ is to determine the number of off-diagonal elements of either type.

Consider baseline 12. The number of baselines that involve antenna 1, but excluding baseline 12 itself, is $n-2$. Likewise, the number of baselines that involve antenna 2, but excluding baseline 12, is also $n-2$. Thus for any *given* baseline such as 12 there are $2(n-2)$ baselines that share a common station. Since there are n_b baselines, the total number of type a covariance elements is

$$n_1 = 2n_b(n-2). \tag{21a}$$

The number of type b elements is therefore

$$n_2 = (n_b^2 - n_b) - n_1 = n_b(n-2)(n-3)/2, \tag{21b}$$

since the size of the covariance matrix is n_b^2 and the total number of nondiagonal elements is $n_b^2 - n_b$.

With the help of Eqs. (21), the variance at the phase center is

$$V_I(0,0) \sim \frac{(n_b + n_1\mu^a + n_2\mu^b)}{n_b^2}\,\sigma^2_R. \tag{22}$$

In the absence of any correlations between the fringe phasors, $V_I(0,0)$ would be σ^2_R/n_b. This is the usual result and corresponds to a contribution only from the diagonal terms. However, the signal itself introduces some correlations and, in general, the nondiagonal terms also contribute. Let E be the ratio of the contribution of all the nondiagonal terms to that of the diagonal terms. Then,

$$V_I(0,0) = \frac{(1+E)}{n_b}\sigma_R^2, \tag{23}$$

where

$$E = \frac{n_1[S/(S+N)] + n_2[S/(S+N)]^2}{n_b}. \tag{24}$$

For the problem at hand, viz., a point source at phase center, the only useful measurement is that of the flux of the source. The flux is estimated by noting the mean value of the pixel at the phase center. Thus the SNR of the flux measurement is

$$F = \sqrt{\frac{n_b}{1+E}}\left(\frac{S}{\sigma_R}\right), \tag{25}$$

where $\sigma_R = (S+N)/\sqrt{M}$ [see Eq. (12)]. F can thus be regarded as the SNR in the map.

We now study the dependence of F, the SNR in the map, as a function of S.

(i) Weak source (S/N$\ll$1). In this regime, the principal contribution comes from the diagonal terms $E\sim 0$ and $F = \sqrt{n_b}\,(S/\sigma_R)$. Thus the SNR in the map does increase as the square root of the number of baselines.

(ii) Moderate source (S/N$\sim 1/n$). In this regime, the flux intercepted by the *entire* array (nS) is comparable to the receiver-noise equivalent flux density generated by any *one* antenna. From Eqs. (14e) and (16c) we find $\mu^a \sim 1/n$, $\mu^b \sim 1/n^2$, $\sigma_R^2 \sim N/M$. Thus $E\sim 2[(n-2)/n] + 1/2[(n-2)/n][(n-3)/n]$. Thus, in this regime, the nondiagonal terms dominate over the diagonal terms since $E > 1$. In detail, for sources stronger than $S > N/n$, the contribution of the b terms exceeds that of the a terms and likewise for sources weaker than N/n the opposite is true.

(iii) Strong source (S/N$\gtrsim$1). In this regime, E is significantly larger than 1 and most of the noise is coming from the type b terms. For S/N$\sim$1, both μ^a and μ^b are comparable to unity [Eqs. (15b) and (17b)] and thus $E\sim n_b$. Thus $F\sim M$, independent of S. Such a result is well known in the context of single-dish flux measurements. What is surprising about this result is that this saturation in F occurs even for such moderate values of S/N. The reason this happens is that the relevant quantity is the *total* flux intercepted by the array and not the flux by a single antenna. When S/N$\sim$1, the total flux intercepted by the array exceeds the mean noise power of the array by n. Thus we are already in the very strong source regime.

VI. STATISTICAL PROPERTIES OF THE BISPECTRUM PHASOR

In Sec. V we estimated the SNR in a synthesis image. However, the analysis was made assuming no corruption of the cosmic signal by the atmosphere. In practice, this is not the case. The phase corruption of the atmosphere is a function of the observing frequency. In the IR window, the atmosphere corrupts cosmic signals over baselines as short as 5 m. This corruption is equally severe at radio wavelengths in VLBI where the baselines span the globe. Once the fringe phase becomes heavily corrupted we can no longer use the van Cittert–Zernike theorem, and standard image synthesis becomes impossible. At cm wavelengths, the phase corruption over baselines typical of connected-element interferometers like the VLA is not severe. Synthesis of the image is possible by the application of the van Cittert–Zernike theorem but the dynamic range of the resulting image would be limited.

To overcome the problem of severe phase corruption, Jennison proposed the use of "closure phases" (see Pearson and Readhead 1984). Closure phase is a phase associated with a triangle of stations in much the same way as the standard fringe phase is the phase associated with the vector defined by two antennas. Thus the measurement of a closure phase needs at least three antennas. Let R_{12}, R_{23}, R_{31} be the standard fringe phasors on baselines 12, 23, and 31, respectively. The closure phase of triangle 123 is defined to be

$$\psi_{123} \equiv \theta_{12} + \theta_{23} + \theta_{31}, \tag{26}$$

where θ_{jk} is the observed or the measured fringe phase on baseline jk. Let χ_j be the additional phase introduced by the atmosphere in the rays reaching antenna j. Then clearly,

$$\theta_{jk} = \phi_{jk} + \chi_j - \chi_k. \tag{27}$$

It is fairly straightforward to show that $\psi_{123} = \phi_{12} + \phi_{23} + \phi_{31}$, i.e., the atmospheric phases cancel out completely and the *closure phase depends only on the source structure.*

The closure phase is also the phase of the so-called *bispectrum* or the *triple product* (see Lohmann, Weigelt, and Wirnitzer 1983; Cornwell 1987):

$$B_{123} \equiv R_{12}R_{23}R_{31}. \tag{28}$$

There is no simple relation between B_{jkl} and the synthesized image as there is between R_{jk} and the image. The number of "basic" or "unique" closure phases in an n-element array is only $n_c = (n-1)(n-2)/2$ (see Pearson and Readhead 1984), which is smaller than $n_b = n(n-1)/2$, the total number of phases needed in order to apply the van Cittert–Zernike theorem. To overcome this problem, Readhead and Wilkinson invented the so-called "hybrid mapping" technique which has been widely used to make VLBI images (see Pearson and Readhead 1984 for full details). Briefly, the technique consists of first assuming a model. The observations supply n_c closure phases, and $n_b - n_c$ phases are obtained from the model and a new model is obtained as per the prescription given by Eq. (18). The previous step is repeated with $n_b - n_c$ phases supplied by the current model. The iterations are continued until the process converges.

There are several problems with the hybrid mapping procedure, some conceptual and some technical. Conceptually, the main problem is that the number of closure phases is equal to the number of triangles, $n_t = n(n-1)(n-2)/6$—considerably larger than n_b. However, of these n_t closure phases, only n_c phases are "basic" in the sense that $n_t - n_c$ closure phases can be derived from the n_c phases, e.g., consider a four-element array (Fig. 3) for which $n_b = 6$, $n_c = 3$, $n_t = 4$. There are four triangles: ACB, ABD, BCD, and ACD. The closure phase of triangle ACD is $\psi_{ACD} = \phi_{AC} + \phi_{CD} + \phi_{DA}$, which is equal to the sum of the closure phases $\psi_{ACB} + \psi_{ABD} + \psi_{BCD}$. In fact, one can assume *any* three triangles to be "basic" and derive the closure phase of the remaining triangle. Despite this symmetry, hybrid mapping makes an arbitrary choice of the "basic" triangles. This has always been a source of dissatisfaction from the conceptual viewpoint.

In order to overcome this and other problems, Cornwell and Wilkinson (1981) and Schwab (1980) came up with the idea of self-calibration in which the χ_j are explicitly solved by using the data itself. The condition that the source must

be finite in size and positive throughout apparently provides sufficient constraints to solve for χ_j 's from the data itself! In self-calibration, the phase-closure condition is implicitly satisfied. In addition, since there are no explicit triangles involved, the above-mentioned dissatisfaction with hybrid mapping is completely avoided.

Currently, self-calibration is the method of choice in the radio window. However, self-calibration fails when $R_{jk}/\sigma_{R_{jk}}$, the SNR of the fringe phasor per baseline per coherence integration interval, falls below 3 (Cornwell 1987). In the radio window this happens for weak sources. In the IR window this regime is readily approached because of the extremely short coherent integration interval, $\tau_I \ll 1$ s. In this low-SNR regime, the bispectrum is the best estimator (Cornwell 1987).

There is a fundamental difference between radio and IR interferometry: at radio wavelengths the observable is the fringe phasor, but in the IR, in the weak source limit, *the observable is the triple product and not the fringe phasor.* A similar situation exists at optical wavelengths (see Nakajima *et al.* 1989 for a further discussion of this point). Thus, in this limit, we have no choice but to use a variant of the hybrid mapping method (see Haniff *et al.* 1987 and Nakajima *et al.* 1989 for applications of hybrid mapping for optical data).

Given this situation, we felt it was worthwhile to study the statistical properties of the bispectrum. The analysis presented here also clarifies the conceptual problem of the hybrid mapping method. In this section we follow the same pattern of analysis as in Sec. IV, viz., first derive expressions for the elements of the covariance matrix and then consider the asymptotic limits.

There are some differences with respect to the previous analysis. The size of the covariance matrix is large: $n_t \times n_t \sim n^6$! Also, there are *three* types of off-diagonal covariance elements: covariance of pairs of bispectrum phasors of triangles with

(1) two common antennas (type "i"),
(2) one common antenna (type "ii"),
(3) no common antenna (type "iii").

A brief note: in order to keep the usage of indexes to the minimum, we use a different notation for the baselines. A single index is used for each baseline, as shown in Fig. 1 for a three-antenna array. The disadvantage with this scheme is that the assignment of the single index to a baseline is arbitrary. In Fig. 1, the baseline index for baseline AB is 1, 2 for baseline BC, 3 for baseline CA.

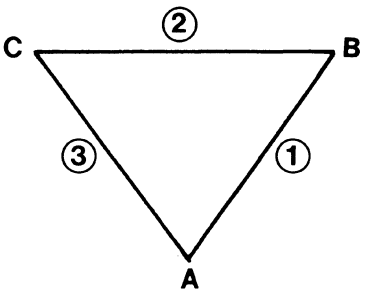

FIG. 1. A three-element array with stations located at A, B, and C. The numbers in open circles denote the baseline indices.

Let us denote by $R_j = A_j e^{i\theta_j}$ the mean complex fringe amplitude measured on baseline 1. A_j is the fringe amplitude and $\theta_j = \phi_j + \chi_j$ is the measured phase; here ϕ_j is the true fringe phase and χ_j is the atmospheric phase. The phase-closure condition is that $\chi_j + \chi_k + \chi_l = 0$ if j, k, and l correspond to baselines that complete a triangle.

In practice, we obtain a series of estimates, denoted by r_j, of the fringe phasor every coherent integration time τ_I (Sec. III). Let r_j^p be the estimate of R_j obtained at $t = p\tau_I$ and q_j^p, the associated measurement noise. In Appendix B, we show the q_j is a complex Gaussian random variable and derive the complete covariance matrix of the fringe phasors. The reader is referred to Appendix B for full results. Here we summarize the statistical properties of q_j:

(1) The mean value of both the real and imaginary components is zero,

$$\langle \mathrm{Re}\,(q_j)\rangle = 0\,,$$
$$\langle \mathrm{Im}\,(q_j)\rangle = 0\,. \tag{29a}$$

(2) Since both Re (q_j) and Im (q_j) are Gaussian variates, the covariance matrix completely defines the statistical properties of the fringe phasor q_j.

$$C\,[\mathrm{Re}\,(q_j),\mathrm{Re}\,(q_j)\,] = \frac{1}{2M}[\,(S+N)^2 + |R_j|^2 \cos\,(2\phi_j)\,] \tag{29b}$$

$$C\,[\mathrm{Im}\,(q_j),\mathrm{Im}\,(q_j)\,] = \frac{1}{2M}[\,(S+N)^2 - |R_j|^2 \cos\,(2\phi_j)\,] \tag{29c}$$

$$C\,[\mathrm{Re}\,(q_j),\mathrm{Im}\,(q_j)\,] = -\frac{1}{2M}|R_j|^2 \sin\,(2\phi_j)$$
$$C\,[\mathrm{Im}\,(q_j),\mathrm{Re}\,(q_j)\,] = C\,[\mathrm{Re}(q_j),\mathrm{Im}\,(q_j)\,]\,. \tag{29d}$$

The pseudovariance $Q_j^2 \equiv \langle q_j q_j^* \rangle$ [cf. Eq. (12)] is

$$Q_j^2 = C\,[\mathrm{Re}\,(q_j),\mathrm{Re}\,(q_j)\,] + C\,[\mathrm{Im}\,(q_j),\mathrm{Im}\,(q_j)\,] = \frac{(S+N)^2}{2B\tau_I}\,. \tag{29e}$$

From Eq. (29d), we note the somewhat surprising result that the real and imaginary components of a fringe phasor are correlated. In retrospect, this result could have been anticipated since the signal is common to both the components. It is convenient to normalize $C\,[\mathrm{Re}\,(q_j),\mathrm{Im}\,(q_j)\,]$ by the pseudovariance Q_j^2 to yield

$$\mu_j \equiv C\,[\mathrm{Re}\,(q_j),\mathrm{Im}\,(q_j)\,]/Q_j^2 = -\left|\frac{R_{12}}{(S+N)}\right|^2 \sin\,(2\phi_j)\,. \tag{29f}$$

In the strong-source limit, $|R_{12}|/(S+N) \sim 1$ and $\mu_j \sim -\sin\,(2\phi_j)$, and, depending upon the source structure, could approach unity. In the weak-source limit, $|R_{12}|/(S+N) \sim S/N$ and $\mu_j \sim (S/N)^2$ and, hence, the cross talk between the real and imaginary components becomes negligible.

(3) The pairwise statistical properties are specified by various covariance elements, $C\,[\mathrm{Re}\,(q_j),\mathrm{Re}\,(q_k)\,]$, $C\,[\mathrm{Re}\,(q_j),\mathrm{Im}\,(q_k)\,]$, $C\,[\mathrm{Im}\,(q_j),\mathrm{Re}\,(q_k)\,]$, and $C\,[\mathrm{Im}\,(q_j),\mathrm{Im}\,(q_k)\,]$ for all j and k. For the purpose of further discussion, it is convenient to characterize the covariance elements: (i) type "a" or type "b" depending upon whether baselines j and k share a common station or not and

(ii) whether the covariance element involves a conjugated pair (i.e., $\mu \propto C[q_j, q_k^*]$) or not (i.e., $\nu \propto C[q_j, q_k]$).

Covariance of fringe phasors with a common station. For specificity, we consider a three-element array with stations at 1, 2, and 3 (Fig. 1). Let the baselines 12, 23, and 13 be represented by $j = 1,2,3$ respectively. Clearly, baselines $j = 1$ and $k = 3$ share a common station. Then in Appendix B we show that

$$\mu_{13}^a \equiv C[q_1, q_3^*]/Q_1 Q_3^* = \frac{R_2^*}{(S+N)}, \tag{29g}$$

$$\nu_{13}^a \equiv C[q_1, q_3]/Q_1 Q_3 = \frac{R_1 R_3}{(S+N)^2}. \tag{29h}$$

Covariance of fringe phasors with no common station. For specificity, we consider a four-element array (Fig. 3). Referring to Fig. 3, we note that baselines 3 and 4 do not share a common station. The two covariance elements for this pair of fringe phasors can be shown to be

$$\mu_{34}^b \equiv C[q_3, q_4^*]/Q_3 Q_4^* = \frac{R_1 R_6^*}{(S+N)^2}, \tag{29i}$$

$$\nu_{34}^b \equiv C[q_3, q_4]/Q_3 Q_4 = \frac{R_5 R_2}{(S+N)^2}. \tag{29j}$$

We assume the atmospheric phase on any antenna to be constant for a certain time $\tau_{\rm coh}$, after which the atmospheric phase is assumed to jump to a random value with uniform probability. We also assume that τ_I is chosen so as to equal $\tau_{\rm coh}$.

From Eqs. (29) it follows that the mean fringe phasor

$$R_j = \langle r_j + q_j \rangle . \tag{30a}$$

Making by now the familiar assumption that temporal and ensemble averages are interchangeable, we see

$$R_j \equiv 1/L \sum_{p=1}^{L} r_j^p + q_j^p , \tag{30b}$$

where L is the total number of measurements of the fringe phasor on baseline j.

In the absence of atmospheric phase corruption, $R_j = \gamma_j S$ and the uncertainty in R_j, $\sigma_{R_j} = Q_j/\sqrt{L} = (S+N)/\sqrt{2Bt}$, where t is the *total* integration time: $t = L\tau_I$. However, owing to the atmospheric phase corruption we expect Eq. (30b) to be equal to zero since

$$\begin{aligned} R_j &= 1/L \sum_{p=1}^{L} r_j^p \\ &= 1/L \sum_{p=1}^{L} A_j\, e^{i\phi_j} e^{i\chi_j^p} \\ &= A_j\, e^{i\phi_j}\, 1/L \sum_{p=1}^{L} e^{i\chi_j^p} = 0 . \end{aligned}$$

It is precisely to overcome this problem that the bispectrum estimator is used.

Consider the bispectrum of the triangle formed by baselines 1, 2, and 3. The mean bispectrum phasor B_{123} is operationally defined as

$$\begin{aligned} B_{123} &\equiv 1/L \sum_{p=1}^{L} \langle b_{123}^p \rangle \\ &= 1/L \sum_{p=1}^{L} \langle (r_1^p + q_1^p)(r_2^p + q_2^p)(r_3^p + q_3^p) \rangle \end{aligned} \tag{31a}$$

$$\begin{aligned} &= 1/L \sum_{p=1}^{L} \langle r_1^p\, r_2^p\, r_3^p \rangle \\ &= 1/L \sum_{p=1}^{L} A_1 A_2 A_3\, e^{i\phi_1 + i\chi_1^p + i\phi_2 + i\chi_2^p + i\phi_3 + i\chi_3^p} \\ &= A_1 A_2 A_3\, e^{i\psi_{123}} (1/L) \sum_{p=1}^{L} e^{i\chi_1^p + i\chi_2^p + i\chi_3^p} \\ &= A_1 A_2 A_3\, e^{i\psi_{123}} , \end{aligned} \tag{31b}$$

since $\chi_1^p + \chi_2^p + \chi_3^p = 0$ for all p.

Parenthetically, we note that the bispectrum estimator is *unbiased* [as demonstrated by Eqs. (31)] *only* in the presence of atmospheric phase corruption. If there was no atmospheric corruption, then Eq. (31a) does not simplify to Eq. (31b) but to

$$\begin{aligned} B_{123} = {} & A_1 A_2 A_3\, e^{i\psi_{123}} + A_1\, e^{i\phi_1} C[q_2, q_3] \\ & + A_2\, e^{i\phi_2} C[q_1, q_3] + A_3\, e^{i\phi_3} C[q_1, q_2] . \end{aligned} \tag{31c}$$

The covariances $C[q_2, q_3]$ etc., are evaluated in Appendix B and are not identically zero because of the finite covariance between the real and imaginary components of the fringe phasor. However, these covariances are $\sim S^2/(2B\tau_I)$ and hence become important only when $(2B\tau_I) \sim 1$—a situation not encountered in any practical interferometer. Thus we conclude that B_{123} is essentially an unbiased estimator.

In Appendix C, we derive the expressions for the variance and the three types of covariance terms. Here we present the results and then study the special case of a point source at the phase center for which $A_j = S$, $Q_j = Q$, $\mu_{jk}^a = \mu^a$, $\mu_{jk}^b = \mu^b$, $\nu_{jk}^a = \nu^a$, and $\psi_{jkl} = 0$, independent of j,k,l; μ^a, μ^b, and ν^a, are real. Here S is the flux density of the point source. The expressions for Q, μ^a, μ^b, ν^a, and ν^b can be found in Eqs. (29).

a) Variance of the Bispectrum

In Appendix C, we show that the pseudovariance of the bispectrum is

$$\begin{aligned} \sigma_{B_{123}}^2 \equiv {} & \langle b_{123} b_{123}^* \rangle - \langle b_{123} \rangle \langle b_{123}^* \rangle \\ = {} & 1/L\, (A_1^2 A_2^2 Q_3^2 + A_1^2 Q_2^2 A_3^2 + Q_1^2 A_2^2 A_3^2 \\ & + A_1^2 Q_2^2 Q_3^2 \{1 + |\mu_{23}^a|^2 + |\nu_{23}^a|^2\} \\ & + Q_1^2 A_2^2 Q_3^2 \{1 + |\mu_{31}^a|^2 + |\nu_{31}^a|^2\} \\ & + Q_1^2 Q_2^2 A_3^2 \{1 + |\mu_{12}^a|^2 + |\nu_{12}^a|^2\} \\ & + Q_1^2 Q_2^2 Q_3^2 \{1 + |\mu_{12}^a|^2 + |\mu_{23}^a|^2 + |\mu_{31}^a|^2 \\ & + O[(\mu^a)^3] + O[\mu^a (\nu^a)^2] + O[\nu^a (\mu^a)^2]\}) . \end{aligned} \tag{32}$$

Equation (32) is a formal and rigorously correct expression for the variance of the bispectrum. Previous estimates (such as the one by Cornwell 1987) are correct only in the asymptotic limit of sources considerably fainter than the receiver noise.

For a point source, Eq. (32) simplifies to

$$\begin{aligned} \sigma_{B_{123}}^2 = {} & 1/L\, (3S^4 Q^2 + 3S^2 Q^4 \{1 + |\mu^a|^2 + |\nu^a|^2\} \\ & + Q^6 \{1 + 3|\mu^a|^2 + O[(\mu^a)^3, (\nu^a)^3]\}) . \end{aligned} \tag{33}$$

We consider two asymptotic limits of Eq. (33).

Faint source ($S \ll Q$). Note that unlike Sec. IV, here we compare the source flux with Q, the uncertainty on the fringe

amplitude, and not N, the receiver-noise power. Note that S/Q is the SNR of the fringe phasor per baseline per coherent integration time. Thus this regime corresponds to the case where the SNR of the fringe-amplitude measurement is below 1. In this limit, $\mu^a \sim 0$ and thus

$$\sigma^2_{B_{123}} = Q^6/L\,, \tag{34a}$$

$$B_{123}/\sigma_{B_{123}} = \sqrt{L}\ (S/Q)^3\,, \tag{34b}$$

identical to the expression derived by Cornwell (1987). Equation (34b) shows that when $S/Q < 1$, the bispectrum is an inferior estimator as compared to the standard fringe phasor. Despite this, we use the bispectrum because, unlike the standard fringe phasor, it is immune to atmospheric phase corruption.

Strong source (S≫Q). In this limit,

$$\sigma^2_{B_{123}} \sim 3S^4Q^2/L\,, \tag{35a}$$

$$B_{123}/\sigma_{B_{123}} \sim \sqrt{\frac{L}{3}}\left(\frac{S}{Q}\right). \tag{35b}$$

The SNR of B_{123} in this limit is only $\sqrt{3}$ worse than the SNR of a single fringe phasor. This is expected because the bispectrum is a product of three random variables. Note that even when $S \gg Q$, but $S \ll N$, μ^a, μ^b, ν^a,ν^b are considerably smaller than unity and hence can be neglected even in this limit.

b) Covariance of Pairs of Bispectrum Phasors with Two Common Antennas

Let 123 and 145 be two triangles with one common side (Fig. 3). Then, in Appendix C we show that the covariance between B_{123} and B_{145} is

$$\begin{aligned} C_{123,145} &= 1/L\,(A_1^2 Q_2Q_3Q_4Q_5(\mu^a_{24}\mu^a_{35} + \mu^b_{25}\mu^b_{34} + \nu^a_{23}\nu^{a*}_{45}) \\ &\quad + A_2A_3A_4A_5Q_1^2 e^{i\psi_{123} - i\psi_{145}} + Q_1^2Q_2Q_3Q_4Q_5 \\ &\quad \times\{\mu^a_{24}\mu^a_{35} + O[(\mu^b)^2] + O[(\nu^b)^2]\}). \end{aligned} \tag{36}$$

For a point source, Eq. (36) simplifies to

$$\begin{aligned} C_{123,145} &= 1/L\,(S^4Q^2 + S^2Q^4 \\ &\quad \times[(\mu^a)^2 + (\mu^b)^2 + (\nu^a)^2] \\ &\quad + Q^6\{(\mu^a)^2 + O[(\mu^b)^2, (\nu^b)^2]\}). \end{aligned} \tag{37}$$

Faint source (S≪Q). We note that in this limit $\mu^a \sim S/N$ and $\nu^a \sim \mu^b \sim (S/N)^2$, both of which are exceedingly small values. Hence, the most dominant term is not Q^6 but S^4Q^2. Thus

$$C_{123,145} \sim S^4Q^2/L, \tag{38a}$$

$$\mu^{(i)}_{123,145} \sim (S/Q)^4, \tag{38b}$$

i.e, the bispectrum phasors B_{123} and B_{145} are essentially uncorrelated. This is expected since the dominant noise in this limit comes from the receiver noise, which is different for triangles 123 and 145 despite the common phasor R_1. The superscript (i) emphasizes that the normalized covariance element is an off-diagonal element of type (i).

Strong source (S≫Q). Keeping the dominant term in S, we note

$$C_{123,145} \sim S^4Q^2/L, \tag{39a}$$

$$\mu^{(i)}_{123,145} \sim 1/3. \tag{39b}$$

Naively we might have expected $\mu^{(i)}$ to be unity in this limit since the incident wave front of a point source is a plane wave front and the voltage samples are exactly the same at all antennas. However, this expectation is not correct because all the derivations in Appendix C including Eq. (36) above have been obtained under the assumption that the atmosphere corrupts the wave front. Thus the assumption of a plane wave front is no longer true. For this reason, the maximum value of $\mu^{(i)}$ is 1/3 since two bispectrum phasors share one common fringe phasor out of the three corrupted fringe phasors that define a bispectrum phasor.

By applying the same logic to the two cases below, we expect $\mu^{(ii)}$ and $\mu^{(iii)}$ to be essentially zero even in the limit of strong sources since there are no common fringe phasors between the pairs of bispectrum phasors with one and no common antenna.

c) Covariance of Pairs of Bispectrum Phasors with One Common Antenna

Let 123 and 456 refer to the triangles with one common antenna (Fig. 4). Then, from Appendix C, we find that

$$\begin{aligned} C_{123,456} &= 1/L\,(Q_1Q_2Q_3Q_4Q_5Q_6\{O[(\mu^a)^2\mu^b] \\ &\quad + O[(\mu^b)^3]\}). \end{aligned} \tag{40}$$

Faint source (S≪Q). Since in this regime, $\mu^a \sim S/N$, $\mu^b \sim (S/N)^2$ we note that the bispectrum phasors are decorrelated in this regime.

$$C_{123,456} \sim Q^6(\mu^a)^2/L, \tag{41a}$$

$$\mu^{(ii)}_{123,456} \sim (\mu^a)^2 \sim 0. \tag{41b}$$

Strong source (S≫Q). Even in this limit, the bispectrum phasors are decorrelated since

$$\mu^{(ii)}_{123,456} \sim 1/3(Q/S)^4(\mu^a)^2, \tag{42}$$

which is essentially zero. As explained in subsec. *b* above, this is expected since the incident wave front is no longer a plane wave front but highly distorted by the atmosphere.

d) Covariance of Pairs of Bispectrum Phasors with No Common Antenna

Let 123 and 456 refer to two triangles with no common vertex (Fig. 5). Then, from Appendix C, we find that

$$\begin{aligned} C_{123,456} &= 1/L\,(Q_1Q_2Q_3Q_4Q_5Q_6 \\ &\quad \times\{O[(\mu^b)^3] + O[(\nu^b)^3]\}). \end{aligned} \tag{43}$$

It is fairly straightforward to show that the bispectrum phasors are decorrelated both in the strong and weak source limits, as in the previous case.

With these results at hand we are now in a position to tackle the question raised at the beginning of this section, viz., "How do we reconcile the much larger number of bispectrum phasors (n_t) with the number of baselines (n_b) or the so called 'unique' phases (n_c)?" Our analysis shows that in fact *all* the bispectrum phasors, i.e., all triangles do provide information. The fact that $n_t > n_b$ should be of no great concern. In the limit of low S/Q the n_t bispectrum phasors provide essentially *independent* information and thus using only a fraction of the bispectrum phasors is equivalent to throwing away valuable data. In the limit of high S/Q the situation is more complex: pairs of bispectrum phasors that share a common side are correlated with $\mu \sim 1/3$ and any other pair is essentially uncorrelated. Thus, even in this regime, all the bispectrum phasors should be used. To con-

clude, both in high and low S/Q limits all the bispectrum phasors provide information and hence should be used in constructing the synthesized image. A corollary conclusion is that the concept of unique closure phases (cf. Pearson and Readhead 1984) is not very useful.

VII. NOISE IN AN IMAGE DERIVED FROM BISPECTRUM DATA

Here we estimate the noise in an image derived from bispectrum data. As mentioned in the beginning of Sec. VI, there is no simple relation between the measured bispectrum phasors and the synthesized image. Currently, all image-construction algorithms employ some kind of an iterative method to obtain images from closure phases. However, when the source structure is simple a simple relation may be possible.

We consider the simplest of all sources, i.e., a point source. This assumption allows some analytical modeling and hence provides new insight into this problem. We believe that the resulting simplification does not hide the essential physics of imaging using bispectrum data. In the case of a point source (assumed to be at the phase center), the only unknown is S, the flux of the source. Thus estimating the uncertainty in the measured values of S is equivalent to obtaining the SNR in the synthesized image.

Let B_j be the bispectrum of triangle j; here, as before, we are using an indexing scheme in which each triangle is given a single index j, which ranges from 1 to n_t. An estimate of the flux from the measured bispectrum phasors is

$$\hat{S} = \mathrm{Re}\,(T)^{1/3}, \tag{44}$$

where $T \equiv \langle t \rangle$ and

$$t \equiv 1/n_t \sum_{j=1}^{n_t} b_j. \tag{45}$$

For a point source of flux density S, $T = S^3$. We now estimate the SNR of T. The SNR of $\hat{S}$ is 3 times larger than that of T.

The variance of T is given by

$$\sigma_T^2 = 1/n_t^2 \sum_{j=1}^{n_t} \sum_{k=1}^{n_t} \sigma_{B_j} \sigma_{B_k} \mu(B_j, B_k), \tag{46}$$

where $\sigma_{B_j}^2$ is the variance of B_j [Eq. (32)] and $\mu(B_j, B_k)$ is the normalized covariance between the bispectrum phasors B_j and B_k and specified by Eqs. (36)–(43), depending upon whether B_j and B_k share two, one, or no common antennas, respectively.

As discussed in Sec. VI, the covariance of bispectrum phasors with only one or no common station is essentially zero for any value of S/Q, whereas the covariance of bispectrum phasors with two common stations [i.e., type (i) pairs] is zero at low values of S/Q but 1/3 at high values of S/Q. Thus most elements of the $n_t \times n_t$ covariance matrix are zero other than the n_t diagonal terms, which are unity by definition and $n^{(i)}$ nondiagonal terms which represent pairs of triangles with one common side. Since we are considering a point source, $\sigma_{B_j} = \sigma_B$ and $\mu^{(i)}(B_j, B_k) = \mu^{(i)}$, i.e., independent of j,k. Thus Eq. (46) can be simplified

$$\sigma_T^2 = \left(\frac{n_t + n^{(i)} \mu^{(i)}}{n_t^2} \right) \sigma_B^2. \tag{47}$$

We now estimate $n^{(i)}$. Consider an n-element array and focus on triangle 123. The number of triangles that include side 12, other than triangle 123, is $n - 3$. Likewise, the number of triangles that share sides 23 and 13 is also $n - 3$ for each. Thus, for each *given* triangle we find $3(n-3)$ triangles that share a common side. Since there are n_t triangles, the total number of triangles that share a common side is $n^{(i)} = 3(n-3)n_t$. Thus Eq. (47) becomes

$$\sigma_T^2 = \left[\frac{1 + 3(n-3)\mu^{(i)}}{n_t} \right] \sigma_B^2. \tag{48}$$

Thus the variance of T and hence of $\hat{S}$ depends critically upon $\mu^{(i)}$.

Faint source (S≪Q). In this limit, $\mu^{(i)} \sim 0$ [Eq. (38b)], $\sigma_B = Q^3$ [Eq. (34a)], and hence

$$\sigma_T^2 = Q^6/n_t, \tag{49a}$$

$$T/\sigma_T = \sqrt{n_t}\,(S/Q)^3, \tag{49b}$$

$$\hat{S}/\sigma_{\hat{S}} = 3(T/\sigma_T) = 3\sqrt{n_t}\,(S/Q)^3. \tag{49c}$$

Thus the SNR of T is $\sqrt{n_t}$ better than the SNR of a single bispectrum phasor. This is a restatement of the fact that all the bispectrum phasors are essentially uncorrelated in this regime. Despite this, the SNR of $\hat{S}$ (whose SNR is proportional to that of T) is not as good as in a phase-coherent interferometer because of the factor $(S/Q)^3$, which is considerably less than unity in this regime.

Strong source (S≫Q). In this limit, $\mu^{(i)} \sim 1/3$ [Eq. (39b)], $\sigma_B^2 = 3S^4Q^2$, and hence

$$\sigma_T^2 = \frac{3(n-2)}{n_t} S^4 Q^2, \tag{50a}$$

$$T/\sigma_t = \frac{1}{\sqrt{3}} \sqrt{\frac{n_t}{(n-2)}} \frac{S}{Q} = \sqrt{\frac{n(n-1)}{18}} \frac{S}{Q}, \tag{50b}$$

$$\hat{S}/\sigma_{\hat{S}} = \sqrt{n_b}\,\frac{S}{Q}. \tag{50c}$$

Equation (50c) compares favorably well with the SNR in the map of a phase-coherent interferometer [Eq. (25)]. Thus, when the fringe is readily detected, the use of a bispectrum leads to a final SNR that is *as good as that obtained with an ideal phase-coherent interferometer.*

VIII. APPLICATIONS TO VLA, VLBA, AND IR INTERFEROMETRY

The principal goal of this paper has been a systematic development of the statistical properties of noise in a synthesis image. We now apply the theory developed in this paper to three examples: the VLA, VLBI, and IR interferometry.

a) VLA

The VLA is an array of 27 antennas, each 25 m in diameter (Thompson *et al.* 1980). It presently operates from 1 cm to nearly 100 cm. Currently, in the 5 GHz window, the receiver noise of a typical antenna is 480 Jy. However, new developments in receiver technology are expected to reduce this. In Fig. 2, we plot the SNR in the map for a point source as a function of the source flux density S for $N = 84$ Jy; the time bandwidth product M has been assumed to be equal to 10^9. Also plotted in dashed lines is E, the ratio of the contribution of nondiagonal terms to the diagonal terms [see Eq. (24)].

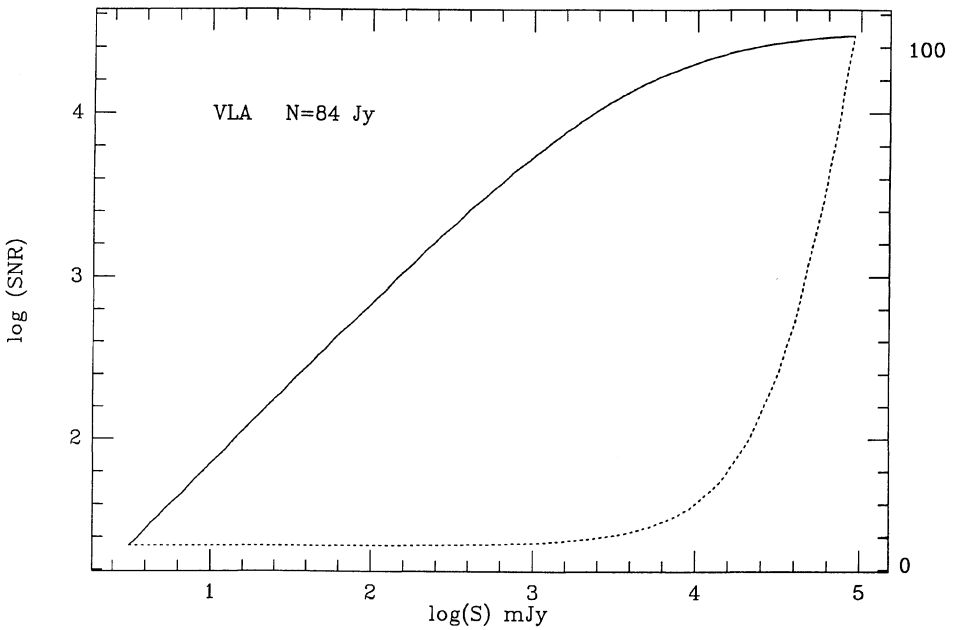

FIG. 2. Plot of signal-to-noise ratio in the synthesized map of a point source as observed by the 27-element VLA (solid line). The noise equivalent flux density or the system noise of each antenna is assumed to be 84 Jy, and the time bandwidth product of a single visibility measurement is assumed to be 10^9. E, the relative ratio of the contribution of nondiagonal terms to the diagonal terms, is shown in dashed lines.

At small values of S, the SNR in the map varies linearly with S. Once $S \sim N/n$, the contribution of the nondiagonal terms exceeds the contribution of the diagonal terms and the growth of the SNR in the map in this region is approximately $S^{1/2}$. Finally, for very strong sources, the SNR in the image is independent of the source flux density and is $\sqrt{2B\tau_1}$.

For the above system, the nondiagonal terms, i.e., the self-noise, contribute about 33% of the total noise for a source with $S \sim 0.851$ Jy. The self-noise linearly increases with source flux density. Thus a source with $S = 6.7$ Jy contributes about 85% of the total noise. At centimeter wavelengths, there are quite a few sources with S comparable to 1 Jy and thus the above example is not an artificial problem. It is fair to state at this point that the self-noise problem is reduced if the source is resolved. Thus, self-noise is unlikely to be important when mapping large extended sources such as Cas A. The self-noise problem becomes more acute at meter wavelength, where the sources are considerably brighter than the centimeter sources and in addition receivers can now be made with essentially negligible electronics noise. This aspect is potentially of some interest to the planned Indian Giant Meter Wavelength Telescope.

It is usually assumed that the noise in a synthesis image is independent of the pixel location. This is a good assumption when the noise arises from the receiver noise since noise generated in one receiver has no effect on the noise generated from other receivers. However, self-noise is noise created by the source itself and hence its distribution *depends upon the source structure itself*. The properties of the noise in the map are formally specified by the covariance matrix,

$$C_I(\theta_x,\theta_y;\theta'_x,\theta'_y) = \langle i(\theta_x,\theta_y) i(\theta'_x,\theta'_y)\rangle - \langle i(\theta_x,\theta_y)\rangle\langle i(\theta'_x,\theta'_y)\rangle, \quad (51)$$

where $i(\theta_x,\theta_y)$ is specified by Eq. (18a). Following the arguments stated in deriving Eq. (19), we find that Eq. (51) can be simplified to

$$\begin{aligned} C_I(\theta_x,\theta_y;\theta'_x,\theta'_y) &= \frac{1}{n_b^2}\sum_{j=1}^{n}\sum_{k>j}^{n}\sum_{j'=1}^{n}\sum_{k'>j'} a_{jk}(\theta_x,\theta_y)a_{j'k'}(\theta'_x,\theta'_y) \\ &\times C[\mathrm{Re}\,(r_{jk}),\mathrm{Re}\,(r_{j'k'})] \\ &+ a_{jk}(\theta_x,\theta_y)b_{j'k'}(\theta'_x,\theta'_y)C[\mathrm{Re}\,(r_{jk}),\mathrm{Im}\,(r_{j'k'})] \\ &+ b_{jk}(\theta_x,\theta_y)a_{j'k'}(\theta'_x,\theta'_y)C[\mathrm{Im}\,(r_{jk}),\mathrm{Re}\,(r_{j'k'})] \\ &+ b_{jk}(\theta_x,\theta_y)b_{j'k'}(\theta'_x,\theta'_y)C[\mathrm{Im}\,(r_{jk}),\mathrm{Im}\,(r_{j'k'})]. \end{aligned} \quad (52)$$

Equation (52) is the complete and formal expression of the covariance matrix of a synthesis image. The variance [cf. Eq. (19)] corresponds to the diagonal elements, i.e., $j = j'$, $k = k'$. The source structure appears in Eq. (52) via the covariance matrix $C_{jk,j'k'}$ (Sec. IV). For sources with $S \ll N/n$, $C_{jk,j'k'}$ is essentially zero for $j \neq j'$ and $k \neq k'$, and in this limit the noise in the synthesized map is white. Once $S \gtrsim N/n$, the covariance matrix C_I has nonzero diagonal elements and the noise is no longer uniform across the map. Further discussion of this problem is beyond the scope of the current paper.

b) Very Long Baseline Interferometry

Currently, VLBI images are obtained from a heterogeneous collection of antennas that span the globe. The array consists of telescopes as small as 25 m to $\lesssim 100$ m antennas. Most of the sources observed with the VLBI array are bright and a fair number are barely resolved. Thus self-noise is potentially a worry in VLBI images.

The theory developed here is really applicable only to antennas with the same aperture size. However, it is quite easy to derive corresponding expressions for an array consisting of heterogeneous antennas. To first order, self-noise becomes important when the flux density of the source becomes comparable to $\bar{N}/n$, where $\bar{N}$ is the *mean* NEFD of the array. Clearly, the NEFD of an array is decreased by the

presence of a large dish. Thus, a VLBI array consisting of five 25 m antennas, two 40 m antennas (OVRO and Green Bank), one 76 m antenna (Jodrell Bank), and two 100 m telescopes (Effelsburg and the WSRT) is equivalent to an array of forty-three 25 m dishes—much larger than the VLA. For such an array, even with current receiver technology, self-noise effects become important for sources as weak as 5 Jy, comparable to many VLBI sources. We urge VLBI observers to carefully evaluate the dynamic range of their best maps and compare it with our predicted noise (cf. Fig. 2). We predict that the dynamic range of the maps of some of the best-observed VLBI sources *may never reach the thermal limit* because of self-noise effects.

Incidentally, the noise properties of the images produced by a heterogeneous array are rather complicated because the covariance elements involving a baseline containing the biggest antenna are larger than the other covariance elements. This aspect again should be of interest to people who are making the highest-dynamic-range maps.

c) IR Interferometry

At the current levels of sensitivity, any IR interferometer employing the heterodyne technique is likely to be in the regime where S/Q is small. In this limit, we have shown that *all* the bispectrum phasors contain independent information. Thus, in our opinion, any image-construction algorithm should make equal use of all the measured bispectrum phasors. As mentioned before, the hybrid mapping method does not treat all the closure phases equivalently. To conclude, we suggest that a technique that iteratively fits the model closure phases and the amplitudes to the observed amplitudes and the observed closure phases is the most optimal method.

IX. SUMMARY OF THE ANALYTICAL RESULTS

In this paper we have systematically developed the statistical properties of noise in synthesis images produced by radio interferometric arrays like the VLA, the VLBA, etc. We recognize that a full reading of the entire paper is time consuming and that most readers are probably interested in the results of our analysis rather than the details. Consequently, at the referee's suggestion, we now summarize our results.

a) Glossary of the Symbols Used in This Paper

Two different schemes are used for referring to baselines. The first one uses a pair of station or element indexes such as jk; here $1 \leqslant j \leqslant n$ and $1 \leqslant k \leqslant n$, where n is the number of elements in an array. This scheme is referred to as the station- or element-based indexing. The second scheme uses a single index which ranges from 1 to $n_b = n(n-1)/2$, the number of baselines; this is referred to as the baseline-based indexing scheme. The former scheme is used in the discussion of the fringe phasors, whereas the latter is used in the discussion of the bispectrum phasors. The total number of bispectrum phasors is denoted by the symbol n_t and is equal to $n(n-1)(n-2)/6$.

The covariance of a pair of random variates x,y is denoted by $C[x,y]$, which is defined to be

$$C[x,y] \equiv \langle xy \rangle - \langle x \rangle \langle y \rangle.$$

The above definition is the same regardless of whether x and y are real or complex variates. The variance is always denoted by the symbol V, i.e.,

$$V[x] \equiv C[x,x] = \langle x^2 \rangle - \langle x \rangle^2.$$

For complex variates, we use a special variance, the so-called pseudovariance, which is always denoted by the symbol σ and is defined as

$$\sigma_z^2 \equiv \langle zz^* \rangle - \langle z \rangle \langle z^* \rangle.$$

In the section on the statistics of the bispectrum we also use the symbol Q_j^2 to denote the pseudovariance of the fringe phasor R_j, i.e., $Q_j^2 \equiv \sigma_{R_j}^2$. The normalization of the covariance terms is different depending upon whether x and y are real or complex numbers. In the first case, the normalization is the standard factor $\sqrt{V[x]V[y]}$, and in the second case the normalization is taken to be $\sigma_x \sigma_y$.

S = flux density of the source.

N = the noise equivalent flux density of an element and equal to $\frac{1}{2}kT_R/\eta A$, where A, η, and T_R refer, respectively, to the collecting area, the aperture efficiency, and the system temperature of a single element.

M = the time bandwidth product of a single visibility measurement and is defined to be $2B\tau_I$, where B is the bandwidth and τ_I is the coherent integration time. Note that M is usually a very large number (10^9).

r_{jk} = the complex fringe phasor on the baseline connecting element j to element k measured over one single coherent integration interval.

r_{jk}^s = Im (r_{jk}).

r_{jk}^c = Re (r_{jk}).

R_{jk} = the average of r_{jk} over many coherent integration intervals. For a point source, $R_{jk} = S$ and the phase $\phi_{jk} = 0$, after proper calibration.

$C^a_{jk,ik}$ = the complex covariance of the noise in the fringe phasors r_{jk} and r_{ik}^*. The superscript "a" stresses the fact that there is a common element between baselines jk and ik.

$\mu^a_{jk,ik}$ = the above covariance term normalized by $\sigma_{R_{jk}} \sigma_{R_{ik}}$.

$C^b_{jk,lm}$ = the complex covariance of the noise in the fringe phasors r_{jk} and r_{lm}. The superscript "b" is taken to mean that baselines jk and lm do not share a common element.

$\mu^b_{jk,lm}$ = the above covariance normalized in the usual fashion.

n_1 = the total number of type "a" covariance elements; equal to $2n_b(n-2)$.

n_2 = the total number of type "b" covariance elements; equal to $n_b(n-2)(n-3)/2$.

From this point on, the symbols pertain to the analysis of the bispectrum phasor. The baseline-based index is exclusively used below.

b_{jkl} = the bispectrum or the triple product of the triangle associated with baselines j, k, l. $b_{jkl} \equiv r_j r_k r_l$. The baselines j, k, l are assumed to form a closed triangle.

A_j = the fringe amplitude on baseline j.

B_{jkl} = the average of the above quantity over many coherent integration intervals; equal to $A_j A_k A_l e^{i\psi_{jkl}}$.

ψ_{jkl} = the phase of the bispectrum B_{jkl}, which is also the closure phase of the triangle associated with baselines j, k, l.

L = the number of coherent integration intervals over which B_{jkl} is obtained.

q_j = the complex noise associated with the fringe phasor on baseline j.

Q_j^2 = another symbol for the pseudovariance σ_{R_j}. Note that this is also the pseudovariance of q_j.

$\sigma^2_{B_{jkl}}$ = the pseudovariance of b_{jkl}.

μ^a_{jk} = the normalized complex covariance of the fringe phasors on baselines j and k; equivalently, $C[q_j,q_k^*]/\sigma_{Q_j}\sigma_{Q_k}$. The superscript "$a$" implies that baselines j and k share a common element.

ν^a_{jk} = the normalized complex covariance of the pair q_j and q_k. Note the difference between ν^a and μ^a.

μ^b_{jk} = the normalized complex covariance of the pair q_j and q_k^*. As before, the superscript "b" implies that baselines j and k do not share a common element.

ν^b_{jk} = the normalized complex covariance of the pair q_j and q_k.

$C_{jkl,j'k'l'}$ = the complex covariance element of the noise associated with the bispectrum vectors b_{jkl} and $b_{j'k'l'}$, i.e., $C[b_{jkl},b^*_{j'k'l'}]$.

$\mu^{(i)}_{jkl,j'k'l'}$ = the above complex covariance element normalized by the pseudovariances $Q_jQ_kQ_lQ_{j'}Q_{k'}Q_{l'}$. The superscript "(i)" should be taken to mean that the two triangles defined by the baseline index jkl and $j'k'l'$ contain exactly one common baseline.

$\mu^{(ii)}_{jkl,j'k'l'}$ = like the above quantity, except that the two pairs of triangles contain exactly one common element.

$\mu^{(iii)}_{jkl,j'k'l'}$ = like the above quantity, except that the two pairs of triangles contain no common element.

At times, we use pseudovariances and normalized covariances without any indexes, e.g., μ^a,ν^b,σ_B, etc. This usage either implies that the particular parameter is independent of the baseline indexes or that the symbol is used in a generic fashion.

b) Results

1) Statistical properties of fringe phasor

We show that the real and imaginary components of the fringe phasor r_{jk} are both Gaussian variates with mean values R^c_{jk} and R^s_{jk} and the following covariance properties:

$$V[r^c_{jk}] = \frac{1}{2M}[(S+N)^2 + |R_{jk}|^2\cos(2\phi_{jk})],$$

$$V[r^s_{jk}] = \frac{1}{2M}[(S+N)^2 - |R_{jk}|^2\cos(2\phi_{jk})],$$

$$C[r^s_{jk},r^c_{jk}] = C[r^c_{jk},r^s_{jk}] = \frac{-|R_{jk}|^2\sin(2\phi_{jk})}{2M},$$

$$\sigma^2_{Rjk} = \frac{(S+N)^2}{M}.$$

The SNR of the fringe amplitude can be conveniently defined to be $R_{jk}/\sigma_{R_{jk}}$. For a point source, $\phi_{jk} = 0$ and $R_{jk} = S$. In the limit of a weak source, $S \ll N$, we recover the well-known result $\sigma_{R_{jk}} = N/\sqrt{M}$, and in the opposite limit of a strong source we again recover the well-known result $\sigma_{R_{jk}} = S/\sqrt{M}$.

In order to derive the variance in a synthesis image, it is necessary to obtain the variance of the fringe phasors as well as the cross talk or the covariance between pairs of fringe phasors. The magnitude of this cross talk depends upon whether the pairs of baselines contain (type "a") or do not contain (type "b") a common element. For either case, we have evaluated the four possible combinations of the covariance elements: $C[r^c_{jk},r^c_{jk}]$, $C[r^c_{jk},r^s_{jk}]$, $C[r^s_{jk},r^c_{jk}]$, and $C[r^s_{jk},r^s_{jk}]$. Rather than reproduce the results once again, we refer the reader to Appendix B [Eqs. (B10)–(B13) and (B16)–(B19)].

Two particular combinations of the above four possible combination vectors are useful for pedantic reasons as well as in the analysis of the statistics of the bispectrum phasor:

$$\mu^a_{12,13} \equiv \frac{C[r_{12},r^*_{13}]}{\sigma_{R_{12}}\sigma_{R_{13}}} = \frac{R^*_{23}}{(S+N)},$$

$$\nu^a_{12,13} \equiv \frac{C[r_{12},r_{13}]}{\sigma_{R_{12}}\sigma_{R_{13}}} = \frac{R_{12}R_{13}}{(S+N)^2},$$

$$\mu^b_{12,34} \equiv \frac{C[r_{12},r^*_{34}]}{\sigma_{R_{12}}\sigma_{R_{34}}} = \frac{R_{13}R^*_{24}}{(S+N)^2},$$

$$\nu^b_{12,34} \equiv \frac{C[r_{12},r_{34}]}{\sigma_{R_{12}}\sigma_{R_{34}}} = \frac{R_{14}R_{32}}{(S+N)^2}.$$

Note that only μ^a is linear in S/N, whereas the other three are quadratic in S/N. All the four covariance terms tend to zero for weak sources ($S \ll N$), the usual situation. However, in the opposite limit, all the covariances tend to unity provided the source is a compact source so that the correlated flux is comparable to S.

2) Variance in the synthesized map

The variance at any pixel (θ_x,θ_y) is

$$\begin{aligned} V[\theta_x,\theta_y] = \frac{1}{n_b^2}\sum_{j=1}^{n}\sum_{k>j}^{n}\sum_{j'=1}^{n}\sum_{j'>k'}^{n} & a_{jk}(\theta_x,\theta_y) \\ & \times a_{j'k'}(\theta_x,\theta_y)C[r^c_{jk},r^c_{j'k'}] \\ & + a_{jk}(\theta_x,\theta_y)b_{j'k'}(\theta_x,\theta_y)C[r^c_{jk},r^s_{j'k'}] \\ & + b_{jk}(\theta_k,\theta_y)a_{j'k'}(\theta_x,\theta_y)C[r^s_{jk},r^c_{j'k'}] \\ & + b_{jk}(\theta_x,\theta_y)b_{j'k'}(\theta_x,\theta_y)C[r^s_{jk},r^s_{j'k'}]. \end{aligned}$$

Note that $\theta_x = 0, \theta_y = 0$ corresponds to the center, or rather the phase center, of the map. Also the normalization of the Fourier transform is so chosen that for a point source at the phase center $I(0,0) = S$. Evaluation of $V[\theta_x,\theta_y]$ requires proper sorting of the elements of the n_b^2 covariance matrix into type "a," type "b," and variance terms. Expressions for these terms can be found in Appendix B.

For the simple case of a point source at the phase center, we can write an exact expression for the variance in the synthesized map. We show that the ratio $F = I(0,0)/\sqrt{V_I[0,0]}$, which is indicative of the SNR in the synthesized map, is given by

$$F = \sqrt{\frac{n_b}{1+E}}\left(\frac{S}{\sigma_R}\right);$$

here $\sigma_R = (S+N)/\sqrt{M}$. The factor

$$E = \frac{n_1[S/(S+N)] + n_2[S/(S+N)]^2}{n_b}$$

is the ratio of the contribution of the nondiagonal terms to that of the diagonal terms in the covariance matrix. We show that in the weak-source limit, $E \sim 0$ and the standard formulas for SNR are recovered. In the moderate-source limit ($S \sim N$), $E \sim 1$ and the noise in the map is doubled due to this cross talk. In the strong-source limit $S \gg N$, $E \sim n_b$ and F no longer depends upon S and depends only on $\sqrt{M}$.

c) Statistical Properties of Bispectrum Phasor

The bispectrum phasor is sixth order in electric field. Thus its probability distribution is necessarily complex and we were unable to derive it. Fortunately, we were successful in deriving all the first and the second moments including the covariance of pairs of bispectrum phasors—quantities that enable us to derive the SNR in maps produced from bispectrum data.

For simplicity, we assume definite values for the indexes of the triangle of baselines. The pseudovariance of B_{123} is

$$\begin{aligned}\sigma^2_{B_{123}} = 1/L\,(&A_1^2A_2^2Q_3^2 + A_1^2Q_2^2A_3^2 + Q_1^2A_2^2A_3^2\\ &+ A_1^2Q_2^2Q_3^2\{1 + |\mu^a_{23}|^2 + |\nu^a_{23}|^2\}\\ &+ Q_1^2A_2^2Q_3^2\{1 + |\mu^a_{31}|^2 + |\nu^a_{31}|^2\}\\ &+ Q_1^2Q_2^2A_3^2\{1 + |\mu^a_{12}|^2 + |\nu^a_{12}|^2\}\\ &+ Q_1^2Q_2^2Q_3^2\{1 + |\mu^a_{12}|^2 + |\mu^a_{23}|^2 + |\mu^a_{31}|^2\\ &+ O[(\mu^a)^3] + O[\mu^a(\nu^a)^2] + O[\nu^a(\mu^a)^2]\}),\end{aligned}$$

where $Q_j^2 = (S+N)^2/M$ for all j. Dropping the index j we note that Q is much less than N since M is a very large number. In the context of the bispectrum, the definition of a strong and a weak source is different from that of the previous discussion: a weak source is $S < Q$. The faintest source for which self-calibration can be applied is $S/Q \gtrsim 3$, and thus the usual radio source observed with the VLA or the VLBA is in the regime of a strong source.

Assuming a point source, the mean value of the $B_{123} = S^3$ and $Q_j = Q$ for all j and the SNR of the bispectrum phasor in the weak-source limit $B_{123}/\sigma_{B_{123}}$ is $\sqrt{L}\,(S/Q)^3$, considerably worse than the SNR of the fringe phasor, which is S/Q. In the strong-source limit ($S \gg Q$) the SNR becomes $\sqrt{L/3}\,(S/Q)$, which is only $\sqrt{3}$ worse than the SNR of a fringe phasor.

The covariance terms, of which there are three types, complete the essential statistical description of the bispectrum phasors:

(i) Pairs of triangles with exactly one common side. Let 123 and 145 be two triangles with one common side (Fig. 3).

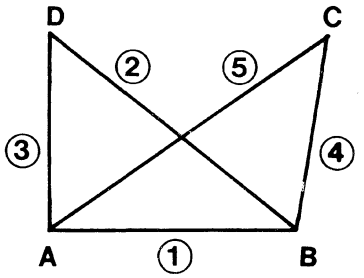

FIG. 3. A four-element array with one common baseline. Numbers in open circles denote the baseline indices. Not all possible baselines are indicated.

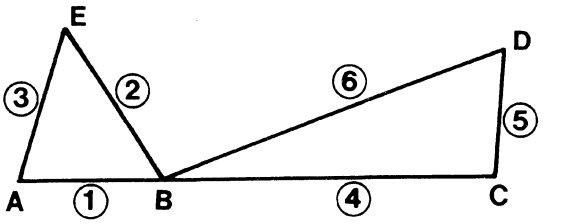

FIG. 4. A six-element array with one common station. Numbers in open circles denote the baseline indices. Not all possible baselines are indicated.

Then the covariance between B_{123} and B_{145} is

$$\begin{aligned}C_{123,145} = 1/L\,(&A_1^2Q_2Q_3Q_4Q_5\{\mu^a_{24}\mu^a_{35} + \mu^b_{25}\mu^b_{34} + \nu^a_{23}\nu^{a*}_{45}\}\\ &+ A_2A_3A_4A_5Q_1^2e^{i\psi_{123} - i\psi_{145}}\\ &+ Q_1^2Q_2Q_3Q_4Q_5\{\mu^a_{24}\mu^a_{35} + O[(\mu^b)^2]\\ &+ O[(\nu^b)^2]\}).\end{aligned}$$

(ii) Pairs of triangles with exactly one common station. Let 123 and 456 refer to the triangles with one common antenna (Fig. 4). Then,

$$\begin{aligned}C_{123,456} = 1/L\,(&Q_1Q_2Q_3Q_4Q_5Q_6\\ &\times\{O[(\mu^a)^2\mu^b] + O[(\mu^b)^3]\}).\end{aligned}$$

(iii) Pairs of triangles with no common station. Let 123 and 456 refer to two triangles with no common vertex (Fig. 5). We find that

$$\begin{aligned}C_{123,456} = 1/L\,(&Q_1Q_2Q_3Q_4Q_5Q_6\\ &\times\{O[(\mu^b)^3] + O[(\nu^b)^3]\}).\end{aligned}$$

The general behavior is that all the normalized covariances tend to zero in the weak-source limit, which is not surprising. In the strong-source limit, the usual situation, $\mu^{(ii)}$ and $\mu^{(iii)}$ are both essentially zero but $\mu^{(i)} \sim 1/3$. This shows that while all triangles provide information, the effective number of bispectrum phasors is less than n_t—an important conclusion of this paper.

By doing an error propagation we show that, at least for the simple case of a point source, the variance of the flux density of a point source inferred from bispectrum data is shown to be

$$\sigma_S^2 = \left[\frac{1 + 3(n-3)\mu^{(i)}}{9n_t}\right]\sigma_B^2.$$

In the weak-source limit, $S/\sigma_S \sim 3\sqrt{n_t}\,(S/Q)^3$, which is considerably worse than the SNR in a map obtained from a

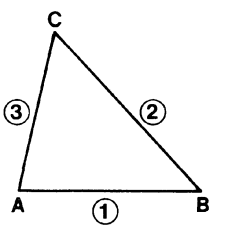

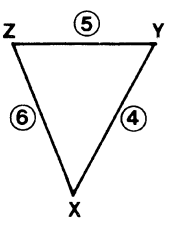

FIG. 5. A four-element array with no common station. Numbers in open circles denote the baseline indices. Not all possible baselines are indicated.

phase-coherent interferometer because S/Q is less than unity. In the strong-source limit, $\mu^{(i)} \sim 1/3$ and the SNR is equal to $\sqrt{n_b}\,(S/Q)$, nearly as good as that obtained from a phase-coherent interferometer.

I am most grateful to the W. M. Keck foundation for a grant under which all of the work reported here was performed. I thank A. C. S. Readhead for early discussions which led to this work, and S. Myers for a careful reading of the manuscript and for pointing out a fundamental flaw with the previous version of the paper. Discussions with D. Jones, T. Nakajima, and T. Pearson were very useful and resulted in improvement of the paper. I thank them for this.

APPENDIX A. FOURTH-ORDER THEOREM FOR COMPLEX GAUSSIAN RANDOM VARIABLES

It is well known that for real Gaussian variables any fourth-order average can be reduced to products of second-order averages (Davenport and Root 1958, p. 168):

$$\langle x_1x_2x_3x_4\rangle = \langle x_1x_2\rangle\langle x_3x_4\rangle + \langle x_1x_3\rangle\langle x_2x_4\rangle + \langle x_1x_4\rangle\langle x_2x_3\rangle. \quad \text{(A1)}$$

In this Appendix, we consider a similar fourth-order average involving complex Gaussian random variables $\langle z_1z_2^*z_3^*z_4\rangle$. Here $z_1 = a_1 + ib_1$, etc., and a_1 and b_1 are zero-mean real Gaussian variables. Thus

$$\langle z_1z_2^*z_3^*z_4\rangle = \langle (a_1 + ib_1)(a_2 - ib_2) \times (a_3 - ib_3)(a_4 + ib_4)\rangle. \quad \text{(A2)}$$

Equation (A2) expands to 16 fourth-order averages: $\langle a_1a_2a_3a_4\rangle$, $i\langle a_1a_2a_3b_4\rangle$, $i\langle a_1a_2b_3a_4\rangle$,...,$\langle b_1b_2b_3b_4\rangle$. Each of these 16 terms can then be expanded to three terms by the use of relation (A1) to yield a total of 48 terms, e.g.,

$$\langle a_1b_2a_3b_4\rangle = C_{12}C_{34} + A_{13}B_{24} + C_{14}C_{32},$$

where $C_{jk} = \langle a_jb_k\rangle$, $A_{jk} = \langle a_ja_k\rangle$, $B_{jk} = \langle b_jb_k\rangle$, etc. By laborious algebra one can show that these 48 terms also correspond to the terms generated by the sum $\langle z_1z_3^*\rangle\langle z_2^*z_4\rangle + \langle z_1z_4\rangle\langle z_2^*z_3^*\rangle$. Thus,

$$\langle z_1z_2^*z_3^*z_4\rangle = \langle z_1z_2^*\rangle\langle z_3^*z_4\rangle + \langle z_1z_3^*\rangle\langle z_2^*z_4\rangle + \langle z_1z_4\rangle\langle z_2^*z_3^*\rangle. \quad \text{(A3)}$$

Thus, the fourth-order theorem for complex signals is identical in form to that for real signals.

However, for a_j, b_j, satisfying the additional relations specified by Eqs. (1) and (2), we can show that terms like

$$\langle z_jz_k\rangle = 0; \quad \text{(A4)}$$

i.e., terms containing no conjugates are zero, in which case

$$\langle z_1z_2^*z_3^*z_4\rangle = \langle z_1z_2^*\rangle\langle z_3^*z_4\rangle + \langle z_1z_3^*\rangle\langle z_z^*z_4\rangle. \quad \text{(A5)}$$

APPENDIX B. STATISTICS OF THE FRINGE PHASOR

In this appendix, we derive the statistical properties of the fringe phasors. We show that, contrary to the assumptions usually found in the literature, the real and imaginary components of the fringe are slightly correlated. This complication forces us to evaluate all possible covariances: real–real, imaginary–imaginary, real–imaginary, and imaginary–real.

Let s_j and n_j be the electrical voltage due to the source and the system, respectively, at antenna j. Since the signals are complex, we represent

$$s_j = a_j + ib_j, \quad \text{(B1)}$$
$$n_j = c_j + id_j.$$

Here, as in Sec. II, we assume that a_j, b_j, c_j, d_j are zero-mean Gaussian random variates with properties specified by relations (1)–(4). As in Sec. II, we note that

$$r_{jk} = \frac{1}{M}\sum_{p=1}^{M}(s_j^p + n_j^p)(s_k^{p*} + n_k^{p*}), \quad \text{(B2)}$$

where $M = 2B\tau_I$ is the number of voltage samples that are used to derive one realization of the fringe phasor, R_{jk}. Letting $r_{jk} \equiv r_{jk}^c + ir_{jk}^s$, we find from Eq. (B2),

$$r_{jk}^c \equiv \mathrm{Re}(r_{jk}) = \frac{1}{M}\sum_{p=1}^{M}[(a_j^p + c_j^p)(a_k^p + c_k^p) + (b_j^p + d_j^p)(b_k^p + d_k^p)] \quad \text{(B3a)}$$

$$r_{jk}^s \equiv \mathrm{Im}(r_{jk}) = \frac{1}{M}\sum_{p=1}^{M}[(b_j^p + d_j^p)(a_k^p + c_k^p) - (a_j^p + c_j^p)(b_k^p + d_k^p)]. \quad \text{(B3b)}$$

As mentioned in Sec. II, the typical value of M is very large. Thus, from the central limit theorem we argue that both r_{jk}^c and r_{jk}^s are Gaussian variables with a mean value of R_{jk}^c and R_{jk}^s; the mean fringe phasor is thus $R_{jk} = R_{jk}^c + iR_{jk}^s$. Once we agree that r_{jk}^c and r_{jk}^s are Gaussian random variates, then the covariance matrix completely characterizes the statistical properties of r_{jk}^c and r_{jk}^s.

Let

$$A_{jk} \equiv \langle a_ja_k\rangle = \tfrac{1}{2}|R_{jk}|\cos(\phi_{jk}), \quad \text{(B4a)}$$
$$B_{jk} \equiv \langle a_jb_k\rangle = \tfrac{1}{2}|R_{jk}|\sin(\phi_{jk}). \quad \text{(B4b)}$$

From relations (1) and (2) we note that

$$\langle b_jb_k\rangle = A_{jk}, \quad B_{jk} = -B_{kj},$$
$$A_{jj} = \tfrac{1}{2}S, \quad B_{jj} = 0, \quad \langle c_jc_j\rangle = \langle d_jd_j\rangle = \tfrac{1}{2}N.$$

Thus,

$$R_{jk}^c \equiv \langle r_{jk}^c\rangle = \frac{1}{M}\sum_{p=1}^{M}[\langle a_j^pa_k^p\rangle + \langle b_j^pb_k^p\rangle] = A_{jk} + A_{kj} = |R_{jk}|\cos(\phi_{jk}), \quad \text{(B5a)}$$

and

$$R_{jk}^s \equiv \langle r_{jk}^s\rangle = \frac{1}{M}\sum_{p=1}^{M}[\langle b_j^pa_k^p\rangle - \langle a_j^pb_k^p\rangle] = B_{kj} - B_{jk} = -|R_{jk}|\sin(\phi_{jk}). \quad \text{(B5b)}$$

a) Covariance Properties of a Single Phasor

The covariance matrix of a single phasor consists of four elements: $C(r_{jk}^c, r_{jk}^c)$, $C(r_{jk}^s, r_{jk}^s)$, $C(r_{jk}^c, r_{jk}^s)$, and $C(r_{jk}^s, r_{jk}^c)$, where $C(x,y) \equiv \langle xy\rangle - \langle x\rangle\langle y\rangle$. We now evaluate these four terms; for specificity we consider baseline 12.

$C(r_{12}^c, r_{12}^c)$ is $V[r_{12}^c]$, the variance of the real component:

$$V[r^c_{12}] \equiv \langle \mathrm{Re}(r_{12})^2 \rangle - \langle \mathrm{Re}(r_{12}) \rangle^2$$
$$= \frac{1}{M^2} \sum_{p=1}^{M} \sum_{q=1}^{M} \langle [(a^p_1 + c^p_1)(a^p_2 + c^p_2) + (b^p_1 + d^p_1)(b^p_2 + d^p_2)] \times [(a^q_1 + c^q_1)(a^q_2 + c^q_2) + (b^q_1 + d^q_1)(b^q_2 + d^q_2)] \rangle - 4A^2_{12}. \quad \text{(B6a)}$$

There are 64 fourth-order averages on the right-hand side of Eq. (B6a): $\langle a^p_1 a^p_2 a^q_1 a^q_2 \rangle, \ldots, \langle d^p_1 d^p_2 d^q_1 d^q_2 \rangle$. Of these, all terms that involve noise components c_1, d_1, c_2, and d_2 are zero unless the noise terms appear in pairs [see Eq. (4)]. Applying the fourth-moment theorem for *real* normal random variates (see Appendix A) and relations (B6), we obtain the following nonzero terms:

$$\langle a^p_1 a^p_2 a^q_1 a^q_2 \rangle = \langle a^p_1 a^p_2 \rangle \langle a^q_1 a^q_2 \rangle + \langle a^p_1 a^q_1 \rangle \langle a^p_2 a^q_2 \rangle + \langle a^p_1 a^q_2 \rangle \langle a^p_2 a^q_1 \rangle$$
$$= A^2_{12} + (\tfrac{1}{2}S)^2 \delta_{pq} + A^2_{12} \delta_{pq},$$
$$\langle a^p_1 a^p_2 b^q_1 b^q_2 \rangle = \langle a^p_1 a^p_2 \rangle \langle b^q_1 b^q_2 \rangle + \langle a^p_1 b^q_1 \rangle \langle a^p_2 b^q_2 \rangle + \langle a^p_1 b^q_2 \rangle \langle a^p_2 b^q_1 \rangle$$
$$= A^2_{12} + B_{12} B_{21} \delta_{pq},$$
$$\langle a^p_1 c^p_2 a^q_1 c^q_2 \rangle = (\tfrac{1}{2}S)(\tfrac{1}{2}N)\delta_{pq},$$
$$\langle c^p_1 a^p_2 c^q_1 a^q_2 \rangle = (\tfrac{1}{2}N)(\tfrac{1}{2}S)\delta_{pq},$$
$$\langle c^p_1 c^p_2 c^q_1 c^q_2 \rangle = (\tfrac{1}{2}N)(\tfrac{1}{2}N)\delta_{pq},$$
$$\langle b^p_1 b^p_2 a^q_1 a^q_2 \rangle = A^2_{12} + B_{12} B_{21} \delta_{pq},$$
$$\langle b^p_1 b^p_2 b^q_1 b^q_2 \rangle = A^2_{12} + (\tfrac{1}{2}S)^2 \delta_{pq} + A^2_{12} \delta_{pq},$$
$$\langle b^p_1 d^p_2 b^q_1 d^q_2 \rangle = (\tfrac{1}{2}S)(\tfrac{1}{2}N)\delta_{pq},$$
$$\langle d^p_1 b^p_2 d^q_1 b^q_2 \rangle = (\tfrac{1}{2}N)(\tfrac{1}{2}S)\delta_{pq},$$
$$\langle d^p_1 d^p_2 d^q_1 d^q_2 \rangle = (\tfrac{1}{2}N)^2 \delta_{pq}.$$

Thus,

$$V[r^c_{12}] = \frac{1}{2M}[(S+N)^2 + |R_{12}|^2 \cos(2\phi_{12})]. \quad \text{(B6b)}$$

Similarly, for the imaginary component,

$$V[r^s_{12}] = \frac{1}{M^2} \sum_{p=1}^{M} \sum_{q=1}^{M} \langle [(b^p_1 + d^p_1)(a^p_2 + c^p_2) - (a^p_1 + c^p_1)(b^p_2 + d^p_2)] \times [(b^q_1 + d^q_1)(a^q_2 + c^q_2) - (a^q_1 + c^q_1)(b^q_2 + d^q_2)] \rangle - 4B^2_{21} \quad \text{(B7a)}$$
$$= \frac{1}{2M}[(S+N)^2 - |R_{12}|^2 \cos(2\phi_{12})]. \quad \text{(B7b)}$$

We find the well-known result that the variances of the real and imaginary components are unequal (cf. Moran 1976). This can be understood from physical reasoning. Assume that the source is a point source at the phase center. Then $\phi_{12} = 0$ and $|R_{12}| = S$. Also assume that $S \gg N$. Then $V[r^c_{12}] = S^2/M$ and $V[r^s_{12}] = 0$. Indeed, this is expected since for a superstrong source ($S \gg N$), the noise in the measurement of the fringe phasor is dominated by the source and, since there is no signal in the quadrature leg, i.e., the imaginary component, $V[r^s_{12}] = 0$.

Now we evaluate the covariance between the imaginary and the real components. Note that $C(r^c_{jk}, r^s_{jk}) = C(r^s_{jk}, r^c_{jk})$ and hence it is sufficient to calculate either one.

$$C[r^c_{12}, r^s_{12}] \equiv \langle r^c_{12} r^s_{12} \rangle - \langle r^c_{12} \rangle \langle r^s_{12} \rangle$$
$$= \frac{1}{M^2} \sum_{p=1}^{M} \sum_{q=1}^{M} \langle [(a^p_1 + c^p_1)(a^p_2 + c^p_2) + (b^p_1 + d^p_1)(b^p_2 + d^p_2)] \times [(b^q_1 + d^q_1)(a^q_2 + c^q_2) - (a^q_1 + c^q_1)(b^q_2 + d^q_2)] \rangle - 4A_{12}B_{21} \quad \text{(B8a)}$$
$$= -\frac{|R_{12}|^2 \sin(2\phi_{12})}{2M}. \quad \text{(B8b)}$$

Thus we find the surprising result that the imaginary and real components are *not independent*. In retrospect, it is clear that the correlation is to be expected via the signal terms.

In Sec. III we defined a variancelike term, $\sigma^2_{R_{12}} \equiv \langle r_{12} r^*_{12} \rangle - R_{12} R^*_{12}$. This "pseudovariance" can be expressed as

$$\sigma^2_{R_{12}} = V[r^c_{12}] + V[r^s_{12}] + iC[r^c_{12}, r^s_{12}] - iC[r^s_{12}, r^c_{12}]$$
$$= \frac{(S+N)^2}{M}. \quad \text{(B9)}$$

Thus, $\sigma^2_{R_{12}}$ is independent of the source structure and in addition receives no contribution from the covariance of the real and imaginary components. Since this pseudovariance is independent of the source structure, we use this term in normalizing the covariance matrix.

b) Covariance Properties of Pairs of Phasors—Common Station

Now we consider the covariance properties of two phasors which share a common baseline: 12 and 13 (for example). Note that unlike the previous case, we have to estimate all four covariance elements: $C[r^c_{12}, r^s_{13}]$, $C[r^s_{12}, r^s_{13}]$, $C[r^s_{12}, r^c_{13}]$, and $C[r^c_{12}, r^s_{13}]$. At this point we simply present the results. The steps used to obtain these elements follow from straightforward extension of the formulation used in the previous section.

$$C[r^c_{12}, r^c_{13}] = \frac{+(N+S)A_{23} + 2A_{13}A_{12} + 2B_{13}B_{21}}{M}, \quad \text{(B10)}$$

$$C[r^s_{12}, r^s_{13}] = \frac{+(N+S)A_{23} - 2A_{13}A_{12} - 2B_{13}B_{21}}{M}, \quad \text{(B11)}$$

$$C[r^c_{12}, r^s_{13}] = \frac{-(N+S)B_{23} + 2A_{13}B_{21} + 2B_{31}A_{12}}{M}, \quad \text{(B12)}$$

$$C[r^s_{12}, r^c_{13}] = \frac{+(N+S)B_{23} + 2A_{13}B_{21} + 2B_{31}A_{12}}{M}. \quad \text{(B13)}$$

For the discussion of the SNR of the bispectrum (Sec. VII) we need to evaluate the following two types of covariance elements: $C[r_{12}, r^*_{13}]$ and $C[r_{12}, r_{13}]$. The former is the covariance between a *conjugated* pair of fringe phasors with a common station, whereas the latter measures the correla-

tion between an *unconjugated* pair of fringe phasors with a common station.

$$C[r_{12},r_{13}^*] = C[r_{12}^c,r_{13}^c] + C[r_{12}^s,r_{13}^s] + iC[r_{12}^c,r_{13}^s] - iC[r_{12}^s,r_{13}^c] = \frac{(N+S)R_{23}^*}{M}, \quad \text{(B14a)}$$

identical to Eq. (14d). Similarly, we get

$$C[r_{12},r_{13}] = C[r_{12}^c,r_{13}^c] - C[r_{12}^s,r_{13}^s] + iC[r_{12}^c,r_{13}^s] + iC[r_{12}^s,r_{13}^c] = \frac{R_{13}R_{12}}{M}. \quad \text{(B14b)}$$

It is convenient to normalize these two covariance elements by the appropriate combination of the pseudovariance $\sigma_{R_{jk}}$:

$$\mu_{12,13}^a \equiv C[r_{12},r_{13}^*]/\sigma_{R_{12}}\sigma_{R_{13}} = R_{23}^*/(S+N), \quad \text{(B15a)}$$

$$\nu_{12,13}^a \equiv C[r_{12},r_{13}]/\sigma_{R_{12}}\sigma_{R_{13}} = \frac{R_{12}R_{13}}{(S+N)^2}; \quad \text{(B15b)}$$

here, as in Sec. IV, the superscript "a" signifies that the covariance element is that of a pair of fringe phasors with a common station. Note that we have used a different symbol, ν, in order to draw the reader's attention to the fact that this element represents the covariance of an unconjugated pair of fringe phasors.

The behavior of the ν terms is qualitatively different from that of the μ terms at low signal strengths. This arises primarily because the covariance elements of the conjugated pairs contain a contribution from the receiver noise, whereas the covariance element of the unconjugated pairs has a contribution only from the astronomical signals. The result is that in the weak-source limit ($S \ll N$), $\mu_{12,13}^a \sim S/N$, $\nu_{12,13}^a \sim (S/N)^2$, and the contribution of the ν terms can be safely ignored in comparison to that of the μ terms.

c) Covariance Properties of Pairs of Phasors—No Common Station

Consider four antennas located at 1, 2, 3, and 4. Then the fringe phasors r_{12} and r_{34} do not share any common station. The four covariance elements of this paper can be shown to be

$$C[r_{12}^c,r_{34}^c] = \frac{+2A_{13}A_{24}+2A_{14}A_{23}+2B_{13}B_{24}+2B_{14}B_{23}}{M}, \quad \text{(B16)}$$

$$C[r_{12}^s,r_{34}^s] = \frac{+2A_{13}A_{24}-2A_{14}A_{23}+2B_{13}B_{24}-2B_{14}B_{23}}{M}, \quad \text{(B17)}$$

$$C[r_{12}^c,r_{34}^s] = \frac{+2B_{13}A_{24}+2B_{41}A_{23}+2A_{13}B_{42}+2A_{14}B_{23}}{M}, \quad \text{(B18)}$$

$$C[r_{12}^s,r_{34}^c] = \frac{-2B_{13}A_{24}+2B_{41}A_{23}-2A_{13}B_{42}+2A_{14}B_{23}}{M}. \quad \text{(B19)}$$

As before, we evaluate the two types of elements of the covariance matrix:

$$\mu_{12,34}^b \equiv C[r_{12},r_{34}^*]/\sigma_{R_{12}}\sigma_{R_{34}} = \frac{R_{13}R_{24}^*}{(S+N)^2}, \quad \text{(B20a)}$$

$$\nu_{12,34}^b \equiv C[r_{12},r_{34}]/\sigma_{R_{12}}\sigma_{R_{34}} = \frac{R_{14}R_{32}}{(S+N)^2}. \quad \text{(B20b)}$$

Two facts are noteworthy: (1) the covariance elements of type "b" do not contain any contribution from receiver noise and (2) both the μ and ν terms scale with signal strength in pretty much an identical fashion, viz., $\propto (S/N)^2$ at low signal strengths. Both of these result from the fact that correlation is induced only via the astronomical signal. Common fluctuations between baselines with no common receiver require simultaneous fluctuations in the remaining two antennas, hence the quadratic behavior at low S/N.

APPENDIX C. VARIANCE AND COVARIANCE OF BISPECTRUM

In this appendix we present detailed calculations leading to the estimation of the variance and the covariance of the bispectrum phasor. As explained in the text, we use a single index for the baselines. While this scheme reduces the clutter in the equation, it has the disadvantage that the assignment of the baseline index is arbitrary. The reader is warned of this pitfall. For the calculations in the first part of this appendix we consider a three-antenna array with the antennas located at A, B, and C (Fig. 1). Baseline indexes 1 through 3 correspond to baselines AB, BC, and CA. The bispectrum phasor is denoted by the symbol B_{jkl}, where j, k, and l are the baseline indexes that form the triangle in question. Thus in Fig. 1, the bispectrum phasor of triangle ABC is B_{123}.

a) Variance of the Bispectrum Phasor

The pseudovariance $\sigma_{B_{123}}^2$ is defined as

$$\sigma_{B_{123}}^2 \equiv \langle b_{123}b_{123}^* \rangle - \langle b_{123}\rangle\langle b_{123}^*\rangle = 1/L^2 \sum_{p=1}^{L}\sum_{q=1}^{L} \langle (r_1^p+q_1^p)(r_2^p+q_2^p)(r_3^p+q_3^p) \times (r_1^{q*}+q_1^{q*})(r_2^{q*}+q_2^{q*})(r_3^{q*}+q_3^{q*})\rangle - |B_{123}^2|. \quad \text{(C1)}$$

There are 64 sixth-order terms in Eq. (C1) ranging from $r_1^p r_2^p r_3^p r_1^{q*} r_2^{q*} r_3^{q*}$ to $q_1^p q_2^p q_3^p q_1^{q*} q_2^{q*} q_3^{q*}$. Of these 64 terms, many average to zero once we realize that $r_j^p = A_j e^{i\phi_j + i\chi_j^p}$, where χ_j^p is the random atmospheric phase on baseline j at $t = p\tau_1$. Thus only terms in which the random atmospheric phase has been cancelled out and terms with no atmospheric terms survive the statistical averaging process. Also, all terms not containing pairs of noise components will average to zero owing to relations (4) and (5). Using these two criteria we find only seven that are nonzero:

$$\langle r_1^p r_2^p r_3^p r_1^{q*} r_2^{q*} r_3^{q*}\rangle = B_{123}B^*_{123},$$
$$\langle r_1^p r_2^p q_3^p r_1^{q*} r_2^{q*} q_3^{q*}\rangle = A_1^2 A_2^2 \langle q_3^p q_3^{q*}\rangle = A_1^2 A_2^2 Q_3^2 \delta_{pq},$$
$$\langle r_1^p q_2^p r_3^p r_1^{q*} q_2^{q*} r_3^{q*}\rangle = A_1^2 Q_2^2 A_3^2 \delta_{pq},$$
$$\langle q_1^p r_2^p r_3^p q_1^{q*} r_2^{q*} r_3^{q*}\rangle = Q_1^2 A_2^2 A_3^2 \delta_{pq},$$
$$\langle r_1^p q_2^p q_3^p r_1^{q*} q_2^{q*} q_3^{q*}\rangle = A_1^2 \delta_{pq} \langle q_2^p q_3^p q_2^{q*} q_3^{q*}\rangle$$
$$= A_1^2 \delta_{pq} (\langle q_2^p q_2^{q*}\rangle \langle q_3^p q_3^{q*}\rangle + \langle q_2^p q_3^{q*}\rangle \langle q_3^p q_2^{q*}\rangle + \langle q_2^p q_3^p\rangle \langle q_2^{q*} q_3^{q*}\rangle)$$
$$= A_1^2 Q_2^2 Q_3^2 [1 + |\mu_{23}^a|^2 + |\nu_{23}^a|^2] \delta_{pq},$$
$$\langle q_1^p r_2^p q_3^p q_1^{q*} r_2^{q*} q_3^{q*}\rangle = Q_1^2 A_2^2 Q_3^2 [1 + |\mu_{31}^a|^2 + |\nu_{31}^a|^2] \delta_{pq},$$
$$\langle q_1^p q_2^p r_3^p q_1^{q*} q_2^{q*} r_3^{q*}\rangle = Q_1^2 Q_2^2 A_3^2 [1 + |\mu_{12}^a|^2 + |\nu_{12}^a|^2] \delta_{pq},$$
$$\langle q_1^p q_2^p q_3^p q_1^{q*} q_2^{q*} q_3^{q*}\rangle = \langle q_1^p q_2^p\rangle (\langle q_3^p q_1^{q*}\rangle \langle q_2^{q*} q_3^{q*}\rangle + \langle q_3^p q_2^{q*}\rangle \langle q_1^{q*} q_3^{q*}\rangle + \langle q_3^p q_3^{q*}\rangle \langle q_1^{q*} q_2^{q*}\rangle)$$
$$+ \langle q_1^p q_3^p\rangle (\langle q_2^p q_1^{q*}\rangle \langle q_2^{q*} q_3^{q*}\rangle + \langle q_2^p q_2^{q*}\rangle \langle q_1^{q*} q_3^{q*}\rangle + \langle q_2^p q_3^{q*}\rangle \langle q_1^{q*} q_2^{q*}\rangle)$$
$$+ \langle q_1^p q_1^{q*}\rangle (\langle q_2^p q_3^p\rangle \langle q_2^{q*} q_3^{q*}\rangle + \langle q_2^p q_2^{q*}\rangle \langle q_3^p q_3^{q*}\rangle + \langle q_2^p q_3^{q*}\rangle \langle q_3^p q_2^{q*}\rangle)$$
$$+ \langle q_1^p q_2^{q*}\rangle (\langle q_2^p q_3^p\rangle \langle q_1^{q*} q_3^{q*}\rangle + \langle q_2^p q_1^{q*}\rangle \langle q_3^p q_3^{q*}\rangle + \langle q_2^p q_3^{q*}\rangle \langle q_3^p q_1^{q*}\rangle)$$
$$+ \langle q_1^p q_3^{q*}\rangle (\langle q_2^p q_3^p\rangle \langle q_1^{q*} q_2^{q*}\rangle + \langle q_2^p q_2^{q*}\rangle \langle q_3^p q_2^{q*}\rangle + \langle q_2^p q_2^{q*}\rangle \langle q_3^p q_1^{q*}\rangle)$$
$$+ \langle q_2^p q_3^q\rangle (\langle q_1^p q_1^{q*}\rangle \langle q_2^{q*} q_3^{q*}\rangle + \langle q_1^p q_2^{q*}\rangle \langle q_1^{q*} q_3^{q*}\rangle + \langle q_1^p q_3^{q*}\rangle \langle q_1^{q*} q_2^{q*}\rangle)$$
$$+ \langle q_2^p q_1^{q*}\rangle (\langle q_1^p q_3^p\rangle \langle q_2^{q*} q_3^{q*}\rangle + \langle q_1^p q_2^{q*}\rangle \langle q_3^p q_3^{q*}\rangle + \langle q_1^p q_3^{q*}\rangle \langle q_3^p q_2^{q*}\rangle)$$
$$+ \langle q_2^p q_2^{q*}\rangle (\langle q_1^p q_3^p\rangle \langle q_1^{q*} q_3^{q*}\rangle + \langle q_1^p q_1^{q*}\rangle \langle q_3^p q_3^{q*}\rangle + \langle q_1^p q_3^{q*}\rangle \langle q_3^p q_1^{q*}\rangle)$$
$$+ \langle q_2^p q_3^{q*}\rangle (\langle q_1^p q_3^p\rangle \langle q_1^{q*} q_2^{q*}\rangle + \langle q_1^p q_2^{q*}\rangle \langle q_3^p q_2^{q*}\rangle + \langle q_1^p q_2^{q*}\rangle \langle q_3^p q_1^{q*}\rangle)$$
$$+ \langle q_3^p q_1^{q*}\rangle (\langle q_1^p q_2^p\rangle \langle q_2^{q*} q_3^{q*}\rangle + \langle q_1^p q_2^{q*}\rangle \langle q_2^p q_3^{q*}\rangle + \langle q_1^p q_3^{q*}\rangle \langle q_2^p q_2^{q*}\rangle)$$
$$+ \langle q_3^p q_2^{q*}\rangle (\langle q_1^p q_2^p\rangle \langle q_1^{q*} q_3^{q*}\rangle + \langle q_1^p q_1^{q*}\rangle \langle q_2^p q_3^{q*}\rangle + \langle q_1^p q_3^{q*}\rangle \langle q_2^p q_1^{q*}\rangle)$$
$$+ \langle q_3^p q_3^{q*}\rangle (\langle q_1^p q_2^p\rangle \langle q_1^{q*} q_2^{q*}\rangle + \langle q_1^p q_1^{q*}\rangle \langle q_2^p q_2^{q*}\rangle + \langle q_1^p q_2^{q*}\rangle \langle q_2^p q_1^{q*}\rangle)$$
$$= Q_1^2 Q_2^2 Q_3^2 \{1 + |\mu_{12}^a|^2 + |\mu_{23}^a|^2 + |\mu_{31}^a|^2$$
$$+ O[(\mu^a)^3] + O[\mu^a(\nu^a)^2] + O[\nu^a(\mu^a)^2]\} \delta_{pq}.$$

In the above derivation, we have shown the full expansion of the various statistical moments for pedantic reasons. In the final analysis, it is sufficient to keep only the most significant terms. The ν^a terms scale as $(S/N)^2$, where S is the source flux density and N is the NEFD of each antenna. Thus we neglect their contribution in comparison to the contribution from the μ^a terms. Adding all these nonzero contributions, we find

$$\sigma^2_{B_{123}} = 1/L\,(A_1^2 A_2^2 Q_3^2 + A_1^2 Q_2^2 A_3^2 + Q_1^2 A_2^2 A_3^2$$
$$+ A_1^2 Q_2^2 Q_3^2 \{1 + |\mu^a|^2 + O[(\nu^a)^2]\}$$
$$+ Q_1^2 A_2^2 Q_3^2 \{1 + |\mu^a|^2 + O[(\nu^a)^2]\}$$
$$+ Q_1^2 Q_2^2 A_3^2 \{1 + |\mu^a|^2 + O[(\nu^a)^2]\}$$
$$+ Q_1^2 Q_2^2 Q_3^2 \{1 + |\mu_{12}^a|^2 + |\mu_{23}^a|^2 + |\mu_{31}^a|^2$$
$$+ O[(\mu^a)^3] + O[\mu^a(\nu^a)^2] + O[\nu^a(\mu^a)^2]\}). \quad \text{(C2)}$$

Note that the noise components are also affected by the atmospheric phase corruption. In the limit of weak source, the noise terms are essentially determined by the receiver noise and thus the phase corruption by the atmosphere does not matter. (We are assuming that the atmosphere does not introduce any gain variations.) In the strong-source limit the noise components are generated by the astronomical signal and, in addition, are getting increasingly correlated [cf. Eqs. (15b) and (17b)]. In this regime, the phase corruption by the atmosphere could lead to decorrelation in the noise terms. However, for the above seven terms that survive the statistical averaging process, the noise components occur pairwise and thus the atmospheric phase is cancelled out. Thus, Eq. (C2) is valid even in the limit of strong sources.

b) Covariance of Pairs of Triangles with Common Side

Consider a four-element array (Fig. 3). Triangles ABC (B_{123}) and ABD (B_{145}) share a common side. In this subsection we estimate the covariance of the bispectrum phasors corresponding to triangles ABC and ABD.

$$C_{123,145} = \langle b_{123} b^*_{145}\rangle - \langle b_{123}\rangle \langle b^*_{145}\rangle$$
$$= 1/L^2 \sum_{p=1}^{L} \sum_{q=1}^{L} \langle (r_1^p + q_1^p)(r_2^p + q_2^p)(r_3^p + q_3^p)$$
$$\times (r_1^{q*} + q_1^{q*})(r_4^{q*} + q_4^{q*})(r_5^{q*} + q_5^{q*})\rangle - B_{123}B_{145}. \quad \text{(C3)}$$

There are 64 sixth-order terms in Eq. (C3) from $r_1^p r_2^p r_3^p r_1^{q*} r_4^{q*} r_5^{q*}$ to $q_1^p q_2^p q_3^p q_1^{q*} q_4^{q*} q_5^{q*}$. Following the logic expounded in subsec. *a* above, only terms where the atmo-

spheric phase has been cancelled out (signal components present pairwise) and terms with no atmospheric terms (only noise terms and no signal) survive the statistical averaging process. Also, owing to relation (5), all terms not containing pairs of noise components are zero. In addition, in this case we have yet another term that survives the statistical process, $q_1 r_2 r_3 q_1^* r_4^* r_5^*$. In this case the phase $r_2 r_3$ is $\psi_{123} - \chi_1$, while the phase of $r_4^* r_5^*$ is $\chi_1 - \psi_{145}$. Thus the overall phase of this term is $e^{i\psi_{123} - i\psi_{145}}$, which is devoid of χ_j. Altogether, four terms are nonzero:

$$\langle r_1^p r_2^p r_3^p r_1^{q^*} r_4^{q^*} r_5^{q^*} \rangle = B_{123} B_{145}^*,$$

$$\langle r_1^p q_2^p q_3^p r_1^{q^*} q_4^{q^*} q_5^{q^*} \rangle = A_1^2 Q_2 Q_3 Q_4 Q_5 [\mu_{24}^a \mu_{35}^a + \mu_{25}^b \mu_{34}^b + \nu_{23}^a \nu_{45}^{a^*}] \delta_{pq},$$

$$\langle q_1^p r_2^p r_3^p q_1^{q^*} r_4^{q^*} r_5^{q^*} \rangle = A_2 A_3 A_4 A_5 Q_1^2 e^{i\psi_{123} - i\psi_{145}} \delta_{pq},$$

$$\langle q_1^p q_2^p q_3^p q_1^{q^*} q_4^{q^*} q_5^{q^*} \rangle = Q_1^2 Q_2 Q_3 Q_4 Q_5 \{\mu_{24}^a \mu_{35}^a + O[(\mu^b)^2] + O[(\nu^a)^2] + O[\mu^a (\mu^b)^2]\} \delta_{pq}.$$

Adding all these nonzero contributions, we find

$$C_{123,145} = 1/L \{A_1^2 Q_2 Q_3 Q_4 Q_5 \{\mu_{24}^a \mu_{35}^a + \mu_{25}^b \mu_{34}^b + \nu_{23}^a \nu_{45}^{a^*}\} + A_2 A_3 A_4 A_5 Q_1^2 e^{i\psi_{123} - i\psi_{145}} + Q_1^2 Q_2 Q_3 Q_4 Q_5 \{\mu_{24}^a \mu_{35}^a + O[(\mu^b)^2] + O[(\nu^b)^2] + O[\mu^a (\mu^b)^2]\}). \quad \text{(C4)}$$

c) Covariance of Pairs of Triangles with One Common Antenna

Consider a six-element array ABCDE (Fig. 5). Triangles ABE and BCD share a common antenna. In this subsection we estimate the covariance of the bispectrum phasors corresponding to triangles ABE (B_{123}) and BCD (B_{456}),

$$C_{123,456} = 1/L^2 \sum_{p=1}^{L} \sum_{q=1}^{L} \langle (r_1^p + q_1^p)(r_2^p + q_2^p)(r_3^p + q_3^p) \times (r_4^{q^*} + q_4^{q^*})(r_5^{q^*} + q_5^{q^*})(r_6^{q^*} + q_6^{q^*}) \rangle - B_{123} B_{456}^*. \quad \text{(C5)}$$

Following the logic explained in subsecs. *a* and *b*, we find that only two terms of the 64 sixth-order terms in Eq. (C5) survive the statistical averaging process and we find

$$C_{123,456} = 1/L \{Q_1 Q_2 Q_3 Q_4 Q_5 Q_6 \{O[(\mu^a)^2 (\mu^b)] + O[(\mu^b)^3]\}). \quad \text{(C6)}$$

d) Covariance of Pairs of Triangles with No Common Antenna

Consider a six-element array ABCXYZ (Fig. 5). Triangles ABC and XYZ do not have a common station. In this subsection we estimate the covariance of the bispectrum phasors corresponding to triangles ABC (B_{123}) and XYZ (B_{456}),

$$C_{123,456} = 1/L^2 \sum_{p=1}^{L} \sum_{q=1}^{L} \langle (r_1^p + q_1^p)(r_2^p + q_2^p)(r_3^p + q_3^p) \times (r_4^{q^*} + q_4^{q^*})(r_5^{q^*} + q_5^{q^*})(r_6^{q^*} + q_6^{q^*}) \rangle - B_{123} B_{456}^*. \quad \text{(C7)}$$

The calculations are identical to subsec. *c* above and only two terms of the 64 sixth-order terms in Eq. (C7) survive the statistical averaging process to yield

$$C_{123,456} = 1/L \{Q_1 Q_2 Q_3 Q_4 Q_5 Q_6 \{O[(\mu^b)^3] + O[(\nu^b)^3]\}). \quad \text{(C8)}$$

REFERENCES

Cornwell, T. J. (1987). Astron. Astrophys. **180**, 269.

Cornwell, T. J., and Wilkinson, P. N. (1981). Mon. Not. R. Astron. Soc. **196**, 1067.

Crane, P. C., and Napier, P. J. (1985). In *Synthesis Imaging*, edited by R. A. Perley, F. R. Schwab, and A. H. Bridle (NRAO, Socorro).

Davenport, W. B., and Root, W. L. (1958). *Random Signals and Noise* (McGraw–Hill, New York).

Haniff, C. A., Mackay, C. D., Titterington, D. J., Sivia, D., Baldwin, J. E., and Warner, P. J. (1987). Nature **328**, 694.

Lohmann, A. W., Weigelt, G., and Wirnitzer, B. (1983). Appl. Opt. **22**, 4028.

Moran, J. M. (1976). In *Methods of Experimental Physics*, Vol. 12C, edited by M. L. Meeks (Academic, New York), p. 228.

Nakajima, T., Kulkarni, S. R., Gorham, P. W., Ghez, A. M., Neugebauer, G., Oke, J. B., Prince, T., and Readhead, A. C. S. (1989). Astron. J. **97**, 1510.

Pearson, T. J., and Readhead, A. C. S. (1984). Annu. Rev. Astron. Astrophys. **22**, 97.

Perley, R. A. (1985). In *Synthesis Imaging*, edited by R. A. Perley, F. R. Schwab, and A. H. Bridle (NRAO, Socorro).

Schwab, F. R. (1980). Proc. SPIE **231**, 18.

Thompson, A. R., Clark, B. G., Wade, C. M., and Napier, P. J. (1980). Astrophys. J. Suppl. **44**, 151.

Thompson, A. R., Moran, J. M., and Swenson, G. W. (1986). *Interferometry and Synthesis in Radio Astronomy* (Wiley, New York).